

June 2020

Biogas Upgrading Via Solid Resin-based Amine Sorbents

Olusola Johnson
University of South Florida

Follow this and additional works at: <https://digitalcommons.usf.edu/etd>

 Part of the [Chemical Engineering Commons](#)

Scholar Commons Citation

Johnson, Olusola, "Biogas Upgrading Via Solid Resin-based Amine Sorbents" (2020). *Graduate Theses and Dissertations*.
<https://digitalcommons.usf.edu/etd/8951>

This Thesis is brought to you for free and open access by the Graduate School at Digital Commons @ University of South Florida. It has been accepted for inclusion in Graduate Theses and Dissertations by an authorized administrator of Digital Commons @ University of South Florida. For more information, please contact scholarcommons@usf.edu.

Biogas Upgrading Via Solid Resin-based Amine Sorbents

by

Olusola Johnson

A thesis submitted in partial fulfillment
of the requirements for the degree of
Master of Science in Chemical Engineering
Department of Chemical and Biomedical Engineering
College of Engineering
University of South Florida

Co-Major Professor: John N. Kuhn, Ph.D.
Co-Major Professor: Babu Joseph, Ph.D.
Scott Campbell, Ph.D.

Date of Approval:
June 25, 2020

Keywords: Biofuel, Renewable natural gas, CO₂ adsorption, LFG upgrading, Biomethane

Copyright © 2020, Olusola Johnson

Dedication

I dedicate this work to my biggest supporters, my family. Daddy, FMK, Ma and Grandma, I can't do this without you. Thank you. BJ and Tosin, you guys rocks.

Acknowledgments

I would like to express my deepest gratitude to my advisors, Dr. John Kuhn and Dr. Babu Joseph, for the opportunity to work with them, and for their patience, motivation, enthusiasm, immense knowledge, and continuous support throughout this work. I would like to appreciate the members of the Heterogeneous Catalysis & Materials Chemistry Lab (past and present) for all the help and support. Especially Umadevi, for getting me started on the project, teaching me the experimental procedures and 'Tosin' Sokefun, for running my DRIFTS and always answering my questions.

I would like to gratefully acknowledge the Hinkley Center for Solid and Hazardous Waste Management for funding this project. I would also like to appreciate Dr. Scott Campbell for being part of my committee.

Table of Contents

List of Tables	iii
List of Figures	iv
Abstract	v
Chapter 1: Introduction	1
1.1 Motivation and Problem Statement.....	1
1.2 Research Scope and Thesis Objective	5
1.3 Thesis Outline	6
Chapter 2: Background	8
2.1 Overview of Biogas Upgrading Technologies	8
2.1.1 Physical Absorption	8
2.1.2 Chemical Absorption	9
2.1.3 Pressure Swing Adsorption	10
2.1.4 Membrane Separation	11
2.1.5 Cryogenic Separation	12
2.2 Overview of Amine-Functionalized CO ₂ Adsorbents	15
2.2.1 Silica-based Sorbents	15
2.2.2 Alumina-based Sorbents	16
2.2.3 MOFs-based Sorbents	17
2.2.4 Zeolite-based Sorbents	20
2.2.5 Carbon-based Sorbents	21
2.2.6 Polymeric Resin-based Sorbents	23
2.3 Adsorptive CO ₂ Capture Technologies	23
2.3.1 PSA Process	23
2.3.2 TSA Process	24
2.3.3 Steam Regeneration	26
2.4 Summary	26
Chapter 3: Experimental Evaluation of CO ₂ Separation from Biogas Using PEI-modified Polymeric Resin Sorbent	29
3.1 Experimental Methods	29
3.1.1 Materials	29
3.1.2 Preparation of PEI-Impregnated Resins	29
3.1.3 Characterization of Adsorbents	29
3.1.4 CO ₂ Separation Experiment	30

3.2 Results	32
3.2.1 Characterization of Adsorbents	32
3.2.2 CO ₂ Separation Performance of Adsorbents	36
3.2.3 CO ₂ Adsorption Performance in Humid Conditions	36
3.2.4 Adsorbent Stability Performance	38
3.2.5 Adsorption and Desorption Mechanism	39
Chapter 4: Techno-Economic Analysis of Biogas Upgrading Units Using Supported Amine Sorbents (SAS)	43
4.1 Typical SAS Units Design Conditions	44
4.2 Equation Used	45
4.3 Economic Model	45
4.3.1 Capital Cost/Fixed Capital Investment (FCI) Estimation	45
4.3.2 Operating Cost Calculations	48
4.4 Excel Model Outlook	50
4.5 Results and Discussions	51
4.5.1 Sensitivity Analysis	52
4.5.2 Comparison with Existing Technologies	52
4.5.3 Comparison to Natural Gas	55
Chapter 5: Conclusions and Recommendations	56
References	58
Appendices	66

List of Tables

Table 1.1: Parameter and composition of gases from different sources, impurities and consequences on upgrading technologies	7
Table 2.1: Limitations of the conventional biogas upgrading technologies	14
Table 2.2: CO ₂ adsorption by silica-based amine sorbents	18
Table 2.3: CO ₂ adsorption by alumina-based amine sorbents	19
Table 2.4: CO ₂ adsorption by MOFs-based amine sorbents	21
Table 2.5: CO ₂ adsorption by zeolite-based amine sorbents.....	22
Table 2.6: CO ₂ adsorption by carbon-based amine sorbents.....	24
Table 2.7: CO ₂ adsorption by resin-based amine sorbents	25
Table 2.8: Criteria for evaluating amine sorbent materials for applications	28
Table 3.1: Textural characteristics of HP2MGL and xPEI-HP2MGL	32
Table 3.2: The breakthrough time and adsorption capacities of xPEI-HP2MGL	37
Table 3.3: IR band assignment of PEI-HP2MGL and adsorbed CO ₂	42
Table 4.1: SAS design conditions	46
Table 4.2: Eqn A.1 equipment costing data	47
Table 4.3: Eqn A.2 bare Module Factor Constants	48
Table 4.4: SAS Capital Cost (2019)	53
Table B1: 50PEI-HP2MGL repeatability study	69
Table B2: Experimental Error Calculations	69

List of Figures

Figure 2.1: The investment cost of membrane separation units, amine scrubbers, water scrubbers, pressure swing adsorption units, and physical organic scrubbers.	13
Figure 3.1: Pore size distribution of HP2MGL and xPEI-HP2MGL	33
Figure 3.2: FT-IR spectra of different samples.	35
Figure 3.3: (a) CO ₂ adsorption isotherm of HP2MGL and xPEI-HP2MGL	35
Figure 3.4: (a) CO ₂ adsorption capacity of different loading of amine on HP2MGL	37
Figure 3.5: CO ₂ adsorption capacities of 30PEI-HP2MGL under various moisture conditions	38
Figure 3.6: CO ₂ adsorption capacity of 30PEI-HP2MGL during adsorption-desorption cycles in simulated 3.8%-humid biogas conditions	39
Figure 3.7: The CO ₂ in-situ DRIFTS spectra of 30PEI-HP2MGL	41
Figure 4.1: An illustrative process model for a SAS unit for CO ₂ separation from biogas	44
Figure 4.2: Excel data input tab	50
Figure 4.3: Excel result tab	50
Figure 4.4: Biogas annual upgrading cost breakdown (a) APTES-SBA15 (b) PEI-HP2GML	51
Figure 4.5: Sensitivity results.	53
Figure 4.6: Capital investment cost of different upgrading technologies.	54
Figure 4.7: Cost for biogas upgrading for methane (PSA, water scrubbing and amine scrubbing data)	54
Figure C1: Sorbents pictorial views	70

Abstract

Biogas is a valuable renewable energy generated from anaerobic digestion of biodegradable organic matter. It is applicable as fuel in vehicles, for the generation of electricity, industrial heating, or as raw material to produce chemicals, liquid fuels, syngas, and compressed natural gas (CNG). Carbon dioxide (CO₂) and methane (CH₄) are the major components in biogas, with a trace amount of contaminants, including hydrogen sulfide (H₂S), water vapor (H₂O), nitrogen (N₂), ammonia (NH₃), oxygen (O₂), carbon monoxide (CO), halides, volatile organic compounds (VOCs), siloxanes, and hydrocarbons.

The source of biogas, which is anaerobic digestion of different organic matter or landfill decomposition, determine the presence and quantities of contaminants. Separation of CO₂ from CH₄ is necessary for increasing the heating value of biogas prior to use as a vehicle fuel or for natural gas grid injection. Adsorptive CO₂ technology via solid porous adsorbents is regarded as a promising technique for separating CO₂ from biogas because of low energy demand and small capital investment in comparison to conventional biogas upgrading methods such as ammonia, water, or amine solvent absorption. Porous materials such as activated carbon (AC), zeolite, metal-organic frameworks (MOFs), covalent organic frameworks (COFs), and mesoporous silica has been extensively researched in for application in CO₂ separation technology.

Recently, amine-functionalized silica has been proposed as a sorbent for CO₂. The objective of this thesis is to evaluate its potential for use with biogas upgrading. We synthesized

PEI-impregnated HP2MGL adsorbent for the separation of carbon dioxide from biogas for upgrading to biomethane. The effects of loadings, adsorption, and regeneration were studied. The sorbent exhibited the highest adsorption capacity of $2.73 \text{ mmol}_{\text{CO}_2}/\text{g}_{\text{ads}}$ at 30% amine mass loading, with negligible CH_4 adsorbed in simulated biogas experiments, proving a high affinity towards CO_2 over CH_4 . The saturation capacity of the sorbent increased to $2.92 \text{ mmol}_{\text{CO}_2}/\text{g}_{\text{ads}}$ in the presence of moisture. The sorbent was regenerated completely at 100°C . In the presence of water, the sorbent remains stable over at least five adsorption-desorption cycles. Adsorption and desorption mechanism study under the in-situ CO_2 DRIFTS study proves that CO_2 adsorption on PEI-impregnated sorbent is consistent with the zwitterion reaction mechanism. Desorption of adsorbed CO_2 species from amine occurs by removal of weakly adsorbed species by reduction of CO_2 partial pressure and by removal of the ammonium-carbamate ions via temperature increase to 100°C for desorption of strongly bonded CO_2 molecules from amine surface.

Techno-economic sensitivity analyses show that the amine-functionalized sorbent does not only provide the technical capacity to satisfy the requirement on gas quality, but it also provides a reduction in energy consumption in addition to cost minimization. The PEI-HP2MGL sorbent used for the process achieved economic viability with natural gas at adsorption capacity of $2.7 \text{ mmol}_{\text{CO}_2}/\text{g}_{\text{ads}}$ and 2000 regeneration cycles. PEI-modified polymeric resin is an attractive choice for biogas upgrading to biomethane through CO_2 -adsorptive technology from the experimental and economic feasibility study.

Chapter 1: Introduction

1.1 Motivation and Problem Statement

A broad international consensus has regarded greenhouse gas emissions as the cause of environmental degradation (notably, increasing global warming activity) and the biggest threat to the sustainable development of the world economy. The majority of atmospheric GHGs emissions, which include gases such as carbon dioxide (CO₂), methane (CH₄), nitric oxides (NO_x), fluorinated gases, and Sulphur oxides, are rising due to human activity, accounting for about three-quarter of global GHG impact¹.

Currently, global energy consumption is the source for more than 65 percent of the GHGs emissions². Based on the United States Energy Information Administration projections, the world energy demand will rise by nearly half by 2050.³ Worldwide renewable energy production is required to climb by 3.1% per year between this period to combat energy production shortage due to the dwindling fossil-based energy source growth³.

The amount of GHGs in the atmosphere has risen to about 430 parts per million (ppm) of CO₂ equivalent global warming potential (GWP) in the past years,⁴ from 330 ppm in 1975⁵, raising the global surface temperature by 1°C.⁶ On current trends, the global GHGs could increase to 550 ppm CO₂ eq., which is double the pre-industrial level, by 2050, increasing the average earth temperature by 2- 3°C by 2050 on the earliest⁷.

The 2015 Paris agreement by the UNFCCC 21st Conference of Parties (COP21) established the goal to limit the increase in global warming below 2°C above the pre-industrial level by 2100, with a specific 1.5 °C goal for 2050.⁸ One significant source of greenhouse gases is biomass waste degradation. The U.S produced 254 million wet tons of municipal solid waste (MSW) in 2015, and only 34% of the generated waste was recycled⁹. Of the remaining 66% of generated waste, 80% was discarded in landfills, while 20% was combusted or incinerated.

In 2010, EPA estimated 24% of global emission comes from the agricultural sector (crop cultivation and livestock rearing), and deforestation.¹⁰ Carbon sequestration of dead organic matter, biomass, and soils prevent the emission of carbon dioxide from the atmosphere, therefore offsetting about one-fifth of GHG emissions from the agricultural sector.¹¹ According to the US Energy Information Administration, management of animal waste and burning of crop residue accounts for 28% of GHG emissions in the agricultural sector.¹² The organic matter in the MSW and agricultural waste is converted to biogas (landfill gas) through anaerobic digestion in the digester system (landfill for LFG).

Biogas is a mixture of gases (mainly methane and carbon dioxide) that are produced by anaerobic degradation of organic compounds. Biogas depending on the source organic matter, may contain trace species as well, including water (H₂O), hydrogen sulfide (H₂S), nitrogen (N₂), oxygen (O₂), ammonia (NH₃), carbon monoxide (CO) and hydrogen (H₂).¹³ Furthermore, typical biogas may contain siloxanes, aromatic and halogenated compounds, and dust particles, but the quantities of trace elements present are meager compared to methane and carbon dioxide. Biogas produced from landfills has even more complex mixtures, which include halides, volatile organic compounds (VOCs), and siloxanes¹⁴ in additions to components of biogas. The typical

composition of biogas from landfill and anaerobic digester is compared to natural gas, the effect of the impurities on its utilization, and the natural gas grid injection requirement are presented in Table 1.1.

Methane emission from waste landfills alone was estimated at 148 MMT (million metric tons) CO₂ equivalents (CO₂ eq.) in the United States in 2015, which makes it the third-largest anthropogenic methane source¹⁵. The 2018 Intergovernmental Panel on Climate Change (IPCC) framework recommended swift, comprehensive and atypical changes in all societal sectors, particularly; energy, buildings, cities, industries, and transport to limit global warming to 1.5 °C. The assessment requires carbon dioxide emissions from anthropogenic sources reduces by 45% by 2030, reaching 'net zero' around 2050¹⁶.

Methane recovered from landfill gas is applicable as vehicle fuel production via Fischer-Tropsch synthesis, electricity generation, and injection into natural gas grid^{17, 18}. With global waste production expected to increase by 33 percent through 2050¹⁹, the utilization of biogas as a renewable energy source will significantly reduce anthropogenic GHGs emissions and provide a means to meet the increasing global energy demand. Carbon dioxide is a recalcitrant gas and a major constituent of biogas that reduces the density and heating value of the biogas. Contaminative components of biogas must be separated prior to its utilization for the production of liquid fuels, compressed natural gas (CNG), electricity generation, and industrial heating.

There are two steps involved in this process: biogas cleaning and biogas upgrading. The separation of impurities, such as sulfides and halides from the biogas stream, is biogas cleaning and is performed before the biogas upgrading step. In contrast, biogas upgrading involves carbon

dioxide removal to boost the heating value of biogas to the optimum quality, and the product is bio-methane/Renewable Natural Gas (RNG). The 2010 International Energy Agency (IEA) 'BLUE Map,' recommends different approaches to accomplish a CO₂ emission cap of fourteen gigatons required to achieve the 2 °C global warming target²⁰.

The IEA considers carbon capture from significant point sources such as landfills, amongst the most critical single reduction approaches globally, with a contribution of about eight gigatons, requiring the deployment of existing and new low-cost carbon capture technologies²⁰. Pressure swing adsorption, water scrubbing, membrane separation, cryogenic separation, and others, are carbon dioxide separation techniques used in the past, but it is heavily laden by severe challenges. The disadvantages of using conventional carbon dioxide separation technologies include; (i) inefficient energy processes, (ii) fouling problems in pipelines, (iii) decreased efficiencies because of the high temperatures required for the regeneration step, and (iv) high pressures compressors account for a large portion of both the capital and operating expenses, which presents a significant economic viability challenge to landfill operators and other municipalities.

Adsorptive carbon dioxide separation technologies, particularly amine-modified materials from LFG has generated interest and optimism among researchers and industry alike recently. The large-scale adoption of this technology is dependent on its economic viability. Sorbent materials are required to possess excellent CO₂ adsorptive properties, which include (i) high CO₂ adsorption capacity at the desired design temperature, (ii) higher CO₂ selectivity, (iii) fast adsorption kinetics, and (iv) be regenerable while exhibiting excellent stability over many thousands of cycles and cost-effectiveness to achieve economic feasibility and viability.²¹

Therefore, there is a need for the development of technology with low energy consumption and equipment cost. The goal of this thesis is to investigate the potential for the application of amine-modified sorbents for CO₂ separation from biogas.

1.2 Research Scope and Thesis Objective

The scope of this work is limited to synthesis, characterization, testing of PEI-modified resin for adsorption of CO₂ in different flow conditions, and economic feasibility analysis of the use of PEI-modified resin and APTES-functionalized silica sorbent in carbon dioxide separation from biogas. The flow conditions are limited to pure CO₂, dry, and humid simulated biogas and real biogas conditions. The amine-impregnated resin was tested for cyclic stability only in simulated wet biogas and actual biogas conditions.

The goal of the thesis is to examine the application of amine-modified adsorbent for carbon dioxide separation from biogas. Polyethyleneimine-impregnated resin is the focus of this work. The optimum amine loading for maximum CO₂ uptake in simulated biogas (gas mixtures of CO₂ and CH₄) was evaluated. The CO₂ uptake capacity of the optima sorbent in pure carbon dioxide and simulated dry and wet biogas mixture was studied. CO₂ adsorption isotherms at different amine loading were examined.

The CO₂ adsorption and desorption mechanism was studied. The impact of moisture on the CO₂ uptake capacity and cyclic stability was investigated. The sorbent regenerability and stability was examined by performing multiple adsorption-desorption cycles. Based on the experimental data obtained, a detailed techno-economic analysis of the APTES-functionalized silica sorbent and PEI-modified resin sorbent was performed. Process design and process-

economic calculations were done to examine the economic viability of the process in comparison to conventional carbon capture technologies.

1.3 Thesis Outline

The thesis document organization is as follows; Chapter 2 covers an in-depth background and literature study on biogas upgrading technologies and carbon dioxide capture via amino-supported materials. Chapter 3 highlights carbon dioxide separation from biogas using polyethyleneimine-modified polymeric resin sorbent. Chapter 4 describes process economic studies of biogas upgrading units using supported amine sorbents, including APTES-functionalized Silica sorbent and PEI-modified resin. Finally, Chapter 5 provides the summary and conclusions of the thesis findings and recommendations for future work in biogas upgrading.

Table 1.1: Parameter and composition of gases from different sources, impurities, and consequences on upgrading technologies. The United States, California vehicle, and grid inject requirement. ²²⁻²⁵

Parameter	Unit	Biogas from AD	Landfill Gas	Natural gas	Vehicle and grid injection	Effect of impurity on biogas utilization
Lower heating value	MJ/Nm ³	23	16	40		
	KWh/Nm ³	6.5	4.4	11		
	MJ/Kg	20	12.3	47		
Density	Kg/Nm ³	1.1	1.3	0.84		
Relative density		0.9	1.1	0.63		
Upper Wobbe index	MJ/Nm ³	27	18	55	47.6-56.5	
Methane number		>135	>130	73		
Methane (CH ₄)	Vol%	60-70	35-65	85-92	70-98	
Heavy hydrocarbons	Vol%	0	0	9		
Water vapor (H ₂ O)	Vol%	1-5	1-5			Fouling of engines, compressors, and gas storage tanks due to reaction H ₂ S, NH ₃ , CO ₂ , to form acids.
Carbon dioxide	Vol%	30-40	15-40	0.2-1.5	3	Reduces calorific value and anti-knock properties, and can foul the engine/pipeline.
Nitrogen	Vol%	0-0.5	1.5	0.3-1.0		
Oxygen	Vol%	0	1		<0.2	Susceptible to explosion and corrosion of engines
Hydrogen Sulphide	Ppm	0-400	0-100	1.1-5.9	88	Poisoning of the catalytic converter, engine fouling, and health hazards. Emissions of SO ₂ , SO ₃
Ammonia (NH ₃)	Ppm	100	5	0	<0.0001	Reduces anti-knock fuel properties and causes fouling of engines.
Halide	mg/Nm ³	0-5	20-200		<0.1	Corrosion in engines.
Siloxane	mg/Nm ³		0.82-4	0	0.1	Fouling of engines and catalytic poisoning

Chapter 2: Background

Currently, the removal of CO₂ from biogas produced from anaerobic digester or landfill is done industrially via different physically and chemically based technologies. Their application depends on the technology readiness level and commercial availability. Today's biogas upgrading market is dominated by physical absorption (water and organic solvents scrubbing), amine absorption, membrane separation, pressure swing adsorption, and cryogenic separation.

2.1 Overview of Biogas Upgrading Technologies

2.1.1 Physical Absorption

The physical absorption is where liquid (water and organic solvent) is used as a selective absorbent in the separation of CO₂ and other impurities from biogas. The differential aqueous solubilities of various components in a liquid solution is the principle of separation via the physical absorption method. About forty-one percent of the worldwide biogas upgrading market is attributed to water scrubbing because the technique is less sensitive to impurities in biogas.²⁶ The solubility of methane is twenty-six times lower at room temperature than carbon dioxide.²⁷

Water scrubbing is an energy-intensive technique which requires the availability of high-quality, low-cost water supply. Pall/Raschig are used to pack columns in water scrubbing for effective mass transfer.²² CO₂ absorption is typically carried out in a pressurized environment (6-20 bar).¹⁴ In the desorption column, regeneration of used water is performed with either air or

steam at lower pressure.²² Gas compression, recirculation pumps, and water regeneration cumulated in the process's energy consumption. H₂S poisoning and fouling are avoided by constant water purging.

Methanol and polyethylene glycol-based solvents are organic solvents that exhibit a stronger affinity for acid gases such as CO₂ and H₂S than H₂O, are also employed in CO₂ removal. Commercialized adsorbent, Selexol[®], which is made up of different polyethylene glycol di-methyl ethers, is five times more selective towards carbon dioxide than water²⁸. As a result, this allows for reduced absorbent recycling rates and plant sizing, leading to a reduction in operating and investment costs.²⁴ Consistently, methane content of about 98% with 2% methane losses and high purity CO₂ is achievable in an optimized full-scale plant at 96-98% technical availability with comparative energy consumption as in water scrubbing.^{17, 26} Organic solvents have only 6% of biogas upgrading market shares despite the advantages of technology maturity.²⁶

2.1.2 Chemical Absorption

Chemical absorption is the use of reactive systems for removing CO₂ from biogas. This technology work like a physical absorption method, but there is a chemical reaction between the absorbent amines and CO₂ molecules. CO₂ reactive absorbents amines (monoethanolamine (MEA)), dimethylethanolamine (DMEA), and aqueous alkali solutions (NaOH, KOH, FeCl₂, Fe(OH)₃, K₂CO₃) are often deployed in chemical scrubbing technologies.²⁹ Methane recovery in this technology is higher than 99% with little to no losses in methane (0.1-1.2%). Operationally, water and amine scrubbing is very similar except for the regeneration process.

Regeneration of amine solutions is achieved with steam stripping or temperature swing, and it has high CO₂ purity of about 93% recovered in the process.³⁰ High energy requirements due to the absorbent regeneration, amine foaming, salt precipitation, and amine poisoning by O₂ are the significant disadvantages of this technology.²² The demerits have reduced the application of chemical absorption to only 22% of the worldwide biogas upgrading market share.²⁶

2.1.3 Pressure Swing Adsorption

Pressure swing adsorption operates via the selective adsorption of CO₂ over CH₄ at high pressure on porous sorbent materials. Activated carbon and charcoal, synthetic resins, and zeolites are high surface area materials often used to maximize gas-adsorbent contact.¹⁷ Adsorbent materials can be irreversibly poisoned by H₂S, meaning it has to be separated from biogas before the PSA process.

Vertical columns packed with sorbents are used for the PSA process. The process involves a sequence of adsorption, depressurization, desorption, pressurization, and then the regeneration of the molecular sieves.²² Pressurized raw biogas (4-10 bar) are fed into the vertical column. The column bed adsorbed CO₂, whereby CH₄ flow through the sorbents bed unretained in the column. After bed saturation with CO₂, the feed is shut, and bed pressure reduced to ambient pressure. CO₂ desorb from the sorbent into a CO₂-rich gas stream is released from the adsorber. The adsorber is regenerated and re-pressurized again with raw biogas.¹⁷ Several columns can be linked together to improve biomethane purity and recoveries of about 98% methane and biogas upgrading unit availabilities of 94-96%.^{17, 31} Patterson et al. estimated that PSA has about 21% of the global biogas upgrading market share.^{26, 32}

2.1.4 Membrane Separation

Membranes are dense, selective filters/barriers that can separate fluid components down to the molecular level. Landfill gas upgrading had been employing membranes since the early 1990s.²⁴ Membrane separation involves the selective permeability of gas through a semi-permeable membrane.³¹ It can be a gas-liquid or gas-gas separation membrane. The materials used in gas-liquid separation is a microporous hydrophobic membrane. Gas and liquid molecules flow in opposite directions through the membrane and are separated based on their differential pore differences.²²

In gas-gas separation, such as biogas upgrading, the process takes place at a pressure above 20-40 bar (although some commercial units operate at a pressure of 8-10 bar), leading to about 95% biomethane production.³¹ Membranes used in the separation of carbon dioxide from biogas hold methane and nitrogen while facilitating the diffusion of CO₂, H₂O, O₂, and H₂S through the membrane.¹⁴ Membrane separation (MS) is regarded as a mature technology with technical availability of about 98% accounting for about 10% of the biogas upgrading market share.³²

The investment cost of biogas membrane units is dependent on the design flowrates with up to \$6,500 for flowrates in the range of 100 Nm³/hr.³¹ The operating cost of this technology is primarily reliant on membrane replacement (typically 5-10 yrs lifespan), the cost of gas compression and biogas pretreatment cost (activated carbon replacement plus energy for condensation)³³ The plant maintenance expenses (about 4 % of the capital cost) associated with membrane separation techniques is slightly higher compared to physical and chemical absorption technologies.²³

2.1.5 Cryogenic Separation

This technology uses the differential melting/freezing temperatures of the components of biogas for the removal of water, hydrogen sulfide, and carbon dioxide from methane. The boiling point of CO₂ and CH₄ are -78 °C and -160 °C respectively, leading to carbon dioxide separation by cooling biogas stream at high pressure. N₂, O₂, and siloxanes can be removed from the biogas stream by exploiting their difference in condensation temperatures.³¹ Biogas upgrading via cryogenic method is carried out at constant pressure (usually 10 bar) by sequential cooling to -25 °C, where H₂O, siloxanes, hydrogen sulfide, and halides are separated in their liquid state and then to -55 °C, where carbon dioxide molecules in the liquid state can be removed. The stream is then cooled to -85 °C for the solidification of the remaining carbon dioxide as a polishing step.^{14, 23} The process is operated at elevated pressure to prevent sudden crystallization of carbon dioxide below -78 °C, which prevents pipeline and heat exchange clogging.³¹

Merits of this technology include the production of high purity CO₂ (98%), high-quality methane, and less than 1% methane loss. Although this technology has synergy with the biomethane liquefaction process, it only represents only 0.4% of the upgrading markets globally.^{26, 31} Figure 2.1 compared the specific investment cost of the different technology in relationship with their plant capacity. Table 2.1 summarize the limitations and disadvantages associated with the use of these technologies.

The limitations of the conventional carbon dioxide separation technologies from biogas have driven investigation in the use of alternative carbon separation process in the form of adsorption via both physical and chemical bonding of carbon dioxide to adsorbents.

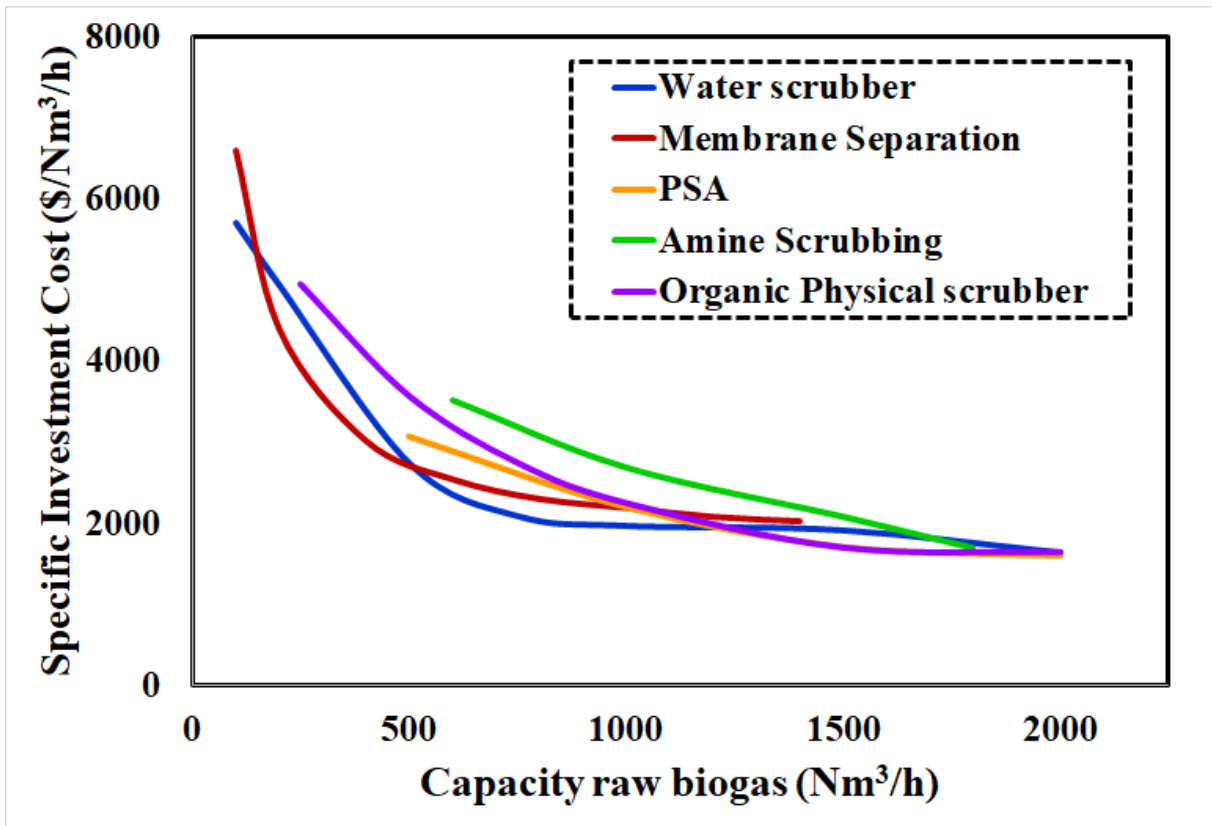


Figure 2.1: The investment cost of membrane separation units, amine scrubbers, water scrubbers, pressure swing adsorption units, and physical organic scrubbers. (Data adapted from Bauer et al³¹)

Several materials such as silica, alumina, zeolites, MOFs, carbons, and porous polymers have been considered for physical adsorption of CO₂ from biogas stream. These physical adsorbents (physiosorbents) utilize van der Waals force interaction, pole-pole, and pole-ions interactions between the CO₂ molecules quadrupole and sorbent's surface polar sites.²¹ Low CO₂ adsorption capacity at ambient pressures, low CO₂ selectivity and preferential water adsorption (in Zeolites) are the most significant limitations of these class of adsorbents.²¹

The incorporation of the CO₂ absorption mechanism via amine solutions into solid adsorbents created a pathway for the chemisorption (a chemical reaction between the CO₂

molecules and the amine group) of CO₂ by amine-functionalized adsorbents. These chemisorbents exhibit high CO₂ adsorption capacity and selectivity at ambient conditions.

Table 2.1: Limitations of conventional biogas upgrading technologies.^{22, 23, 31}

CO₂ separation technologies	Limitations
Physical Adsorption	<ol style="list-style-type: none"> 1. High energy and water/solvent demand 2. Prior H₂S and NH₃ separation required
Chemical Adsorption	<ol style="list-style-type: none"> 1. Relatively expensive 2. High energy consumption 3. Susceptible to corrosion 4. Amine forming and salt precipitation
Pressure Swing Adsorption	<ol style="list-style-type: none"> 1. Prior H₂O and H₂S separation required 2. Multi-stage separation required for high purity gas.
Membrane Separation	<ol style="list-style-type: none"> 1. High methane losses 2. High purity methane-rich gas can be expensive
Cryogenic Separation	<ol style="list-style-type: none"> 1. High energy demand 2. Potential can clog pipeline or heat exchangers

2.2 Overview of Amine-Functionalized CO₂ Adsorbents

2.2.1 Silica-based Sorbents

Since the turn of the century, CO₂ capture via mesoporous silica has been a vast subject area for scientists and researchers. SBA-15, SBA-16, MCM-36, MCM-41, MCM-48, KIT-6, MSU-1, and MSU-J are some of the mesoporous silica been explored as support for amine by researchers. The combination of high surface area, enhanced pore volume, large and adjustable pore diameter³⁴ make these materials highly suitable for amine-functionalization. Generally, amine-functionalization of these materials is via three methods; (i) physical amine impregnation into the pores of the support via van der Waals forces, (ii) aminosilanes grafting onto the support via covalent bonds, (iii) hyperbranched aminosilica materials integrating covalently tethered amines into porous support by Jones et al.,³⁵ and (iv) the combination of methods (i) and (ii) above.

Amine-impregnated adsorbents are synthesized via physically depositing amines into pores of supports by mixing the amine solution with porous supports in solvents accompanied by a drying process for solvent evaporation.²¹ The support and amine interact via van der Waal forces, dipole-dipole interaction, and hydrogen bonding. Adsorption capacity and kinetics are related to the amine loading and the support's textural characteristics. Higher loading in this method may lead to reduced adsorption capacity and slow kinetics due to diffusion and thermodynamic limitation of CO₂ molecules' access to an isolated amine site. Silica-based supports with textural characteristics like larger pore volume and size, shorter pores, and excellent pore connectivity commonly exhibit higher CO₂ adsorption capacities.²¹ Low and high molecular polyethyleneimine (PEI), Monoethanolamine (MEA), tetraethylenepentamine (TEPA),

pentaethylenhexamine (PEHA), diethylenetriamine (DETA), ethylenediamine (EDA), triethanolamine (TEA), triethylenetetramine (TETA), diethanolamine (DEA), and polyallylamine (PAA), among others, have been impregnated on mesoporous silica.

Silica supports due to the presence of surface hydroxyl groups are suitable for amine grafting. Unlike the impregnation methods, according to Jahandar et al., synthesis of the aminosilanes based silica sorbents can be done via; (i) co-condensation of aminosilane and a silica source like tetraethylorthosilicate (TEOS) (ii) aminosilane surface modification of post-synthetic silica.²¹ 3-aminopropyltriethoxysilane (APTES), aminomethyltriethoxysilane, 2-aminoethyltriethoxysilane, 3-aminopropyltrimethoxysilane (APTMS) among others have been grafted on mesoporous silica supports. Higher CO₂ adsorption capacities are achievable on amine-impregnated silicas in comparison with amine-grafted silicas, however diffusional limitations in amine-impregnated silicas mean slower adsorption kinetics.²¹ Weak interaction due to physical bonding between the amine and the supports also results in amine leaching and evaporation, raising concerns over their cyclic stability and long term applications. In order to bridge the advantages of the two classes of materials, the hybrid method has been explored.

2.2.2 Alumina-based Sorbents

Mesoporous alumina materials have a high surface area, large pore volume, and small pore size distributions with CO₂ chemisorption and physisorption surface sites³⁶, making these materials suitable for amine functionalization³⁷. However, limited studies have been done on the use of MA, and only impregnated-MA class have been studied. Chen and Ann impregnated MA with PEI and achieved a CO₂ uptake capacity of 2.73 mmol/g at 75 °C, and 1 bar.³⁸ Various studies

have shown loading of amine on alumina support to be effective in simulated dehumidified and humidified flue gas stream with a CO₂ adsorption capacity of PEI and DEA functionalized γ -alumina, are 1.41³⁹ and 0.68⁴⁰ mmol/g respectively.

2.2.3 MOFs-based Sorbents

Metal-Organic Frameworks (MOFs) are a group of crystalline compounds made up of metal-based nodes, clusters, or ion bridged by organic linkers²¹, which possess high surface area and tunable pore characteristics. These properties made them suitable for amine modification and had been the subject of CO₂ capture. Amino-MOFs can be classified into four types. Type-i materials, because of its large pore volume that allows high concentration amine loading is the most common type, and they are macroporous, unlike mesoporous silica materials.

The porosity of the type-I MOFs allows for both chemisorption and physisorption in practice leading to high CO₂ uptake capacity. However, impregnation of these materials can be complicated by pore blockage from bulky amino polymer due to the materials' pore connectivity and leading to structural decomposition.³⁷ PEI-impregnated MIL-101, ZIF-8 fall under this category. Pokhrel et al. grafted APTES on ZIF-8 to established the first type-II amino-MOFs material.⁴¹ The absence of functionalized sites suitable for silane bonding in MOFs complicates the synthesis procedure.

However, stability in the humidified environment was the advantage gained from this class, although ineffective synthesis procedure renders non-facile candidate for CO₂ capture.³⁷ Energy required for amine-tethering makes type-iii more promising materials than type-ii. Amine is functionalized by attachment to the reactive open metal sites (OMS), influenced by the metallic

Table 2.2: CO₂ adsorption by silica-based amine sorbents

Support	Amine	Amine loading (wt%)	CO ₂ uptake capacity (mmol/g)	Stability test (cycles)	CO ₂ adsorption loss (%)	Ref.
MCM-41	TEPA	40	2.70	10	2	42
MCM-41	PEI (Mn =600)	50	2.05	10	7	43
MCM-48	PEI	50	2.70			44
SBA-15	PEI (Mn = 423)	75	2.00	4	5	45
SBA-15	TEPA	58	3.48	7	19	46
SBA-16	PEI	50	2.93			44
KIT-6	PEI	50	3.07	3	0	44
KIL-2	TEPA	50	4.35			47
MCF	PEI	50	3.45	8	4	48
HMS	PEI	50	2.04	12	15	49
MCM-41	APTES	100	0.70			50
MCM-48	APTES	15	0.479			51

Table 2.2: (Continued)

SBA-15	APTES	50	0.14			52
SBA-15	APTMS	20	1.59			53
SBA-16	AEAPS	15	0.73			54
SBA-16	DETA		0.80			55
SBA-15	Aziridine		3.11			56
PE-SBA-15	AP/TEPA	6/50	4.88			57
KIT-6/ZSM-5	PEI/TMPTA	50/100	4.69			58

Table 2.3: CO₂ adsorption by alumina-based amine sorbents

Support	Amine	Amine loading (wt%)	CO ₂ uptake capacity (mmol/g)	Ref
Mesoporous Alumina	PEI	46.5	2.73	38
γ-alumina	PEI	30	1.41	39
γ-alumina	DEA	36	0.68	40

centers of the MOF.³⁷ Demessence et al. promoted water-stable adsorption through the incorporation of ethyl diamine (ED) into MOF's Cu centers to synthesis high cyclic stable MOFs.⁵⁹ Several type-III MOFs have been reported in the literature, as listed in Table 2.4. Type-IV MOFs represent the class of hybrids of grafting and impregnated method as in mesoporous silica. These increase the CO₂ adsorption capacity and cyclic stability of the materials. Only TEPA-functionalized MIL-101 has been reported by literature in this category.⁶⁰

2.2.4 Zeolite-based Sorbents

Zeolites are microporous aluminosilicate crystalline materials whose framework consists of three-dimensional tetrahedral SiO₄ and AlO₄ configuration.⁶¹ Zeolites are well-suited for gas mixtures separations because of their exceptional surface chemistries, well-defined pore structures, and interconnected pore channels.³⁷ Both synthetic and naturally occurring zeolites have been broadly studied for the carbon dioxide adsorption due to the strong dipole-quadrupole interactions between the zeolitic alkali-metal cations and CO₂ molecules.^{21, 37}

The selectivity of carbon dioxide over nitrogen and methane of amino-zeolites material remains low, disregarding the favorable impacts of the extra framework cations present for adsorption of CO₂ molecules.²¹ Also, water vapor composition in feed gas during CO₂ adsorption has a major negative effect on the CO₂ uptake capacity of Zeolites. Various amine-impregnated or grafted zeolites have been examined for CO₂ capture technology, some of which are listed in Table 2.5 below. Amine-functionalization of zeolites enhances its CO₂ adsorption and selectivity but sacrifices its fast adsorption kinetics at low temperatures due to the diffusional limitation in amine-filled pores of zeolites.⁶²

Table 2.4: CO₂ adsorption by MOFs-based amine sorbents

Support	Amine	Amine loading (wt%)	CO ₂ uptake capacity (mmol/g)	Ref
MIL-101	PEI	100	5.1	63
ZIF-8	PEI	30	1.3	64
MIL-101	TREN	83	3.3	65
HKUST-1	TEPA	8.4	2.6	66
MIL-53	TEPA	7.9	1.4	66
ZIF-8	TEPA	11.5	2.0	66
ZIF-8	APTES	11.8	0.8	41
MIL-101	PEHA	18.9	1.3	67
ZIF-8	ED	2.5	0.68	41

2.2.5 Carbon-based Sorbents

Solidified carbon has been extensively researched as a cheap and abundant material for gas separations. The carbon's physical and chemical properties can be tuned for specific requirements. Aerogels, monoliths, membranes, foams, fibers, particles, or sheets with wide pore structures and surface properties can be made from carbon.²¹ This attribute allows for the synthesis of porous carbon materials such as carbon nanotubes, graphene, activated carbon fibers, carbon molecular sieves, and ordered porous carbons, which have found application in

Table 2.5: CO₂ adsorption by zeolite-based amine sorbents

Support	Amine	Amine loading (wt%)	CO ₂ uptake capacity (mmol/g)	Ref
Zeolite 13X	MEA	50	0.82	62
Zeolite 13X	PEI		1.09	68
Zeolite Y60	TEPA	50	2.56	69
ZSM-5	PEI	40	1.80	70
ZSM-5	TEPA	70	1.49	71
Zeolite β	APTES	40	4.70	72
Zeolite β	TEPA	40	2.55	72
Zeolite β	MEA	40	1.76	73
ITQ-2	APTMS	60	1.73	74
MCM-22	APTMS	60	1.52	74
MCM-36	APTMS	60	1.20	74

CO₂ capture. However, its low CO₂ uptake capacity discouraged its use.

Amine functionalization of carbons is done through the physical amine impregnation, and due to microporosity in carbons, amine-impregnation leads to pore blockage and, ultimately, low

CO₂ adsorption rate.⁷⁵ The pore structure (macroporous or mesoporous) of the support determines the CO₂ uptake performance of the resulting material. Covalent grafting of amine species had notably caused steric hindrance due to the large size of amine compounds such as APTES leading low amine surface density and often low CO₂ capacity.⁷⁶

2.2.6 Polymeric Resin-based Sorbents

Adsorptive resins are classified as porous organic polymers representing a rising type of sorbent material in which building blocks are organic molecules⁷⁷ connected through strong covalent bonds.⁷⁸ Adsorptive resins have high surface area and pore volume, uniform pore size distribution, and distinctive physical attributes (including being spherical shaped), which makes them suitable candidates as support for polyamines.⁷⁹ Adsorptive resins are chemically inert and thermally stable.²² The majority of works in done the utilization of adsorptive resins have been limited to amine-impregnation synthesis methods. Table 2.7 contains a list of resin-based amine sorbents that have been researched for CO₂ capture.

2.3 Adsorptive CO₂ Capture Technologies

2.3.1 PSA Process

In pressure swing adsorption, the most absorbable component of a gas mixture is separated from a feed gas at high pressure, after which the adsorbed species are desorbed from the material. Desorption takes place by decreasing the total system pressure to regenerate the sorbent bed. To meet the vehicle and national grid purity requirement, a multi-stage PSA process is needed, which increases the investment and operational cost of the system. Pressure swing

adsorption is highly desirable for high concentration CO₂ capture from low-volume feed gas streams.²¹

Table 2.6: CO₂ adsorption by carbon-based amine sorbents

Support	Amine	Amine loading (wt%)	CO₂ uptake capacity (mmol/g)	Ref
AC beds	MEA	40	1.11	80
AC	DEA		5.63	81
AC	TEPA		0.90	81
AC	TEA	0.20	0.27	82
AC	AMP	36	1.50	83
AC	AMPD	44	1.20	83
MWCNT	APTES	5	1.25	84
AC	MMEA	36	1.00	83
CM	TAEA	10	1.90	85
GO	ED	50	1.06	86
HG	PEI	42	3.41	87
Mesoporous Carbon	PEI	60	3.8	88

2.3.2 TSA Process

Regeneration via the temperature swing adsorption involves flowing purge gas through the sorbent bed at a temperature above the adsorption temperature to desorb species from the

materials. The availability of heat is a dominant factor in the adoption of this process. Post-combustion CO₂ capture is very suited to the TSA approach due to the abundance of waste heat

Table 2.7: CO₂ adsorption by resin-based amine sorbents

Support	Amine	Amine loading (wt%)	CO ₂ uptake capacity (mmol/g)	Ref
NKA-9	PEI	50	3.43	89
HP20	PEI	50	4.11	90
HP2MGL	PEI	50	4.05	91
XAD-761	PEI	40	3.85	92
D4020	PEI	50	3.20	91
MF	PEI	11.35	1.32	93
XAD-4	TEPA	19	1.21	94
XAD-4	DETA	14	0.69	94
HP2MGL	DEA	50	0.96	91
HP2MGL	DETA	50	1.23	91
PDVB	TEPA	30	1.20	79

for the regeneration process. Most laboratory bench studies use an inert purge gas for the regeneration approach. However, the use of inert purge gas reduces the purity of CO₂ that can be collected downstream.

2.3.2 Steam Regeneration

Generation of high-purity CO₂ for sequestration, enhanced oil recovery, and mineralization, among other applications of CO₂, requires steam stripping of sorbent beds. Steam stripping provides a partial pressure driving force similar to purge gas in TSA and a source of heat for desorption. The stream from the regeneration vessel contains only carbon dioxide and water, which can be easily removed by compressing the CO₂-rich gas and condensing the steam, separating the water in its liquid state to produce a high-purity CO₂-rich gas applicable in mineralization or other commercial use.⁹⁵ Additionally, low-grade steam often considered low-value waste heat, which is a by-product of industrial processes such as electricity-generating power plants or refineries is suitable for regenerating the solid sorbent.

2.4 Summary

In recent years, solid sorbents based on amine either physically impregnated or chemically grafted on porous supports are promising candidates for CO₂ separation have been extensively studied.⁹⁶⁻¹⁰⁴ Solid amine-based sorbents operate at ambient conditions, exhibit fast adsorption and desorption rate, are tolerant to moisture, possess high CO₂ uptake capacity, and is regenerable by mild temperature swings¹⁰⁵.

Based on their different chemical and physical properties, amine adsorbents are classified into different categories¹⁰⁶⁻¹¹² such as Class 1: physically impregnated polymeric amine into porous support, Class 2: covalently grafted amino-silanes, Class 3: covalent grafting of amine polymers on support via in situ polymerization, Class 4: self-supported polyamine adsorbent¹¹³, Class 5: a hybrid of impregnation and grafting methods. High CO₂ working capacity and excellent

cyclic stability of polyethyleneimine (PEI) impregnated-mesoporous silica supports have generated much attention to the type of the sorbents. The CO₂ adsorption performance of these sorbents depends on the morphology of the supports like pore volume⁴⁹, pore size¹¹⁴, and pore connectivity¹¹⁵. Higher pore volume, larger pore size, and excellent pore interconnectivity are characteristics of silica support exhibiting high and improved CO₂ adsorption capacity. Additionally, most PEI-functionalized porous sorbents materials are powders that would have to be pelletized to overcome the disadvantages of material loss due to pressured-gas flow, high-pressure loss, and high energy consumption and high capital cost resulting in high material synthesis cost due to pelletization^{116, 117}.

The use of adsorptive resins supports for solid amine is gaining interest, primarily because they possess adjustable and tunable pores, high CO₂ working capacity, thermal stability (below 130 °c) and are spherically shaped favorable for use in adsorption beds^{90, 92, 118-120}. The separation of CO₂ from the biogas using amine-impregnated polymeric resin had attracted less attention. This work presents an experimental and economic evaluation of utilizing PEI-impregnated resin in biogas upgrading to biomethane via CO₂ adsorption.

Table 2.8: Criteria for evaluating amine sorbent materials for applications.^{13, 14, 23, 37, 121-123}

Utilization yardsticks	Challenges
CO ₂ working capacity	<ol style="list-style-type: none"> 1. High mass-flow rates reduce the dynamic capacities of sorbents 2. Impurities from landfill gas poison sorbents and reduces its capacities
Sorbent kinetics	<ol style="list-style-type: none"> 1. High amine loading lead to diffusional limitations and slow kinetics
Regeneration requirements	<ol style="list-style-type: none"> 1. Unregenerable materials due to chemical adsorption. 2. High regeneration temperature can degrade amine and reduce working capacity
Cost	<ol style="list-style-type: none"> 1. Synthesis cost of Amine-modified materials must be low
Stability	<ol style="list-style-type: none"> 1. Long term cyclic and high-temperature gradient lead to amine degradation

Chapter 3: Experimental Evaluation of CO₂ Separation from Biogas Using PEI-modified Polymeric Resin Sorbent

3.1 Experimental Methods

3.1.1 Materials

Branched Polyethyleneimine (Mw= 1200 Da, 99%) and methanol (>99.5%) were obtained from Polysciences Inc. and Sigma-Aldrich Company, respectively. Commercial adsorption resin, HP2MGL, was bought from Alfa Aesar Chemicals Company.

3.1.2 Preparation of PEI-impregnated Resins

The PEI-impregnated resins were synthesized by the wet impregnation method, as reported in literature⁹¹. The sorbents were labeled as xPEI-HP2MGL after synthesis, where “x” represents the percentage by mass of amine in the adsorbent.

3.1.3 Characterization of Sorbents

N₂ physisorption and CO₂ chemisorption were performed in a Quantachrome Autosorb-iQ at 77K and room temperature (298.15K), respectively, for adsorption-desorption isotherms. The samples were outgassed under vacuum for 5h at 100 °C in both cases. The surface area of samples was calculated within the relative pressure range of 0.05 and 0.3 using the Brunauer–Emmet-Teller (BET) method. The pore size distribution of the samples was examined by the Barrett-Joyner-Halenda (BJH) method to calculate the amount of adsorbed N₂ at a set of relative

pressure (P/P_0) intervals. The desorption branch of the CO_2 isotherm was used to estimate the CO_2 adsorption capacity of the samples. FTIR was performed to examine the different functional groups in the samples with a Thermo-Scientific Nicolet IS50 instrument.

In-situ CO_2 DRIFTS measurement was conducted using a Thermo Scientific Nicolet IS50 spectrometer, which consists of an MCTA detector cooled with liquid nitrogen. 40 mg of the sample was placed on top of 10 mg of KBr powder in a Harrick Scientific reactor cell. Before the analysis, the sample was treated under 20 sccm of argon while heating to 100 °C and held for 30 min at 100. After this treatment, the sample was cooled to 30 °C still under argon flow. During the cool-down process, backgrounds were taken at the following additional temperatures, 90, 80, 70, 60, 50, 40, and 30 °C. Following background collection at 30 °C, a gas mixture consisting of 0.50 sccm CO_2 and 2.5 Ar flowed for 10 min for the CO_2 adsorption/breakthrough experiment. The gas flow was then changed to only argon for 30 min to purge CO_2 from the reaction chamber. After the purging process, at a ramp rate of 10 °C/min, the sample was heated to 100 °C. Sample spectra were taken at the following desorption temperatures at select temperatures between 30 and 100 °C. The spectra were obtained using a resolution of 4 and a data spacing of 0.482 cm^{-1} . The total no of scans obtained was 50.

3.1.4 CO_2 Separation Experiment

Column breakthrough measurements of CO_2 from simulated biogas and LFG separation performance was conducted in fixed bed quartz. The specific CO_2 separation experiment steps are as follows. 2g of the sample was placed in the fixed bed U-tube quartz reactor and pretreated at 100 °C at 10 °C/min and maintained for 2 h in 99.99% He flows to remove all adsorbed gases.

The temperature of the reactor was then reduced to room temperature, and He was switched to the desired gas flow conditions for 30 min for complete sample bed saturation.

A total of 40 sccm of feed gas stream flowed through the adsorbent bed at different conditions: dry conditions (CO₂/He and CO₂/CH₄/He feeds), humid conditions (He/H₂O/CO₂/CH₄ feed gas). Afterward, the bed was reheated to 100 °C (10 °C/min) and fixed for 1 hr in He for sample regeneration. The stability of the adsorbent was tested by repeating the adsorption-desorption cycles. Alicat mass flow controllers controlled all flow to the reactor. The reactor was connected in-line with an MKS Cirrus mass spectrometer (MS) used to analyze the CO₂ concentration in the outflow streams. The CO₂ uptake capacities of sorbents were estimated by the eqn (1):

$$Q_t = \frac{V}{m \cdot G_m} \int_0^t (C_{in} - C_{out}) dt \quad (1)$$

where V is the total feed-gas flow rate, sccm; C_{in} and C_{out} stands for the reactor inflow and outflow CO₂ concentration, vol%; t is the total CO₂ adsorption time, mins. Q_t represents the CO₂ adsorption capacity at saturation when C is equal to C_{in}. G_m is gas molar volume at standard conditions. t_b and Q_b represent the time to breakthrough the bed and the adsorption capacity at breakthrough, respectively.

The accuracy of the adsorption capacity measurement and calculations was determined by repeating the column breakthrough experiment for a sample three times and analyzing the error associated with the experiment. The sample adsorption capacity has a range of 0.05 mmol_{CO2}/g and approximately 1.5% experimental error as calculated.

3.2 Results

3.2.1 Characterization of Adsorbents

The textural characteristics of the pristine and PEI-modified resins are summarized in Table 3.1. As shown in Table 3.1, it is observed that the BET surface area and BJH pore volume of the pristine resin decreased significantly after impregnation and noticeably decreased gradually with increasing PEI loading amount. The mean molecular size of branched PEI of molecular weight 1200 Da is 0.7 nm,¹²⁴ which leads to the increase in the average pore diameter of the sorbent with increasing amine loading. The pore size distribution is present in Figure 3.1 This is mainly due to the amine molecules occupying or blocking the pore channel of the support increasing the channel size of the resin. However, the adsorbent maintains the interfacial area and porosity favorable for kinetic diffusion and adsorption of CO₂ molecules⁹¹.

Table 3.1: Textural characteristics of HP2MGL and xPEI-HP2MGL

Samples	Surface Area (m²/g)	Pore Volume (cm³/g)	Average Pore Diameter (nm)
HP2MGL	587	1.45	18.0
20PEI-HP2MGL	52	0.73	18.0
30PEI-HP2MGL	28	0.62	18.1
40PEI-HP2MGL	16	0.27	18.2
50PEI-HP2MGL	14	0.26	18.4

The FTIR spectra of HP2MGL and xPEI-HP2MGL ($x=20,30,40,50$) is presented in Figure 3.2. For HP2MGL, the broad peak with center at 3440 cm^{-1} was representative of the O–H stretching present due to adsorbed water.⁷⁹ The spectra at 3000 cm^{-1} and 2940 cm^{-1} were characteristic of the C-H stretching vibrations in the polymethacrylate resin^{125, 126}, and the peaks at 1460 cm^{-1} and 1380 cm^{-1} indicate aromatic frame.¹²⁵ In comparison to HP2MGL, some different FTIR spectra peaks were observed in the adsorbent after PEI impregnation.

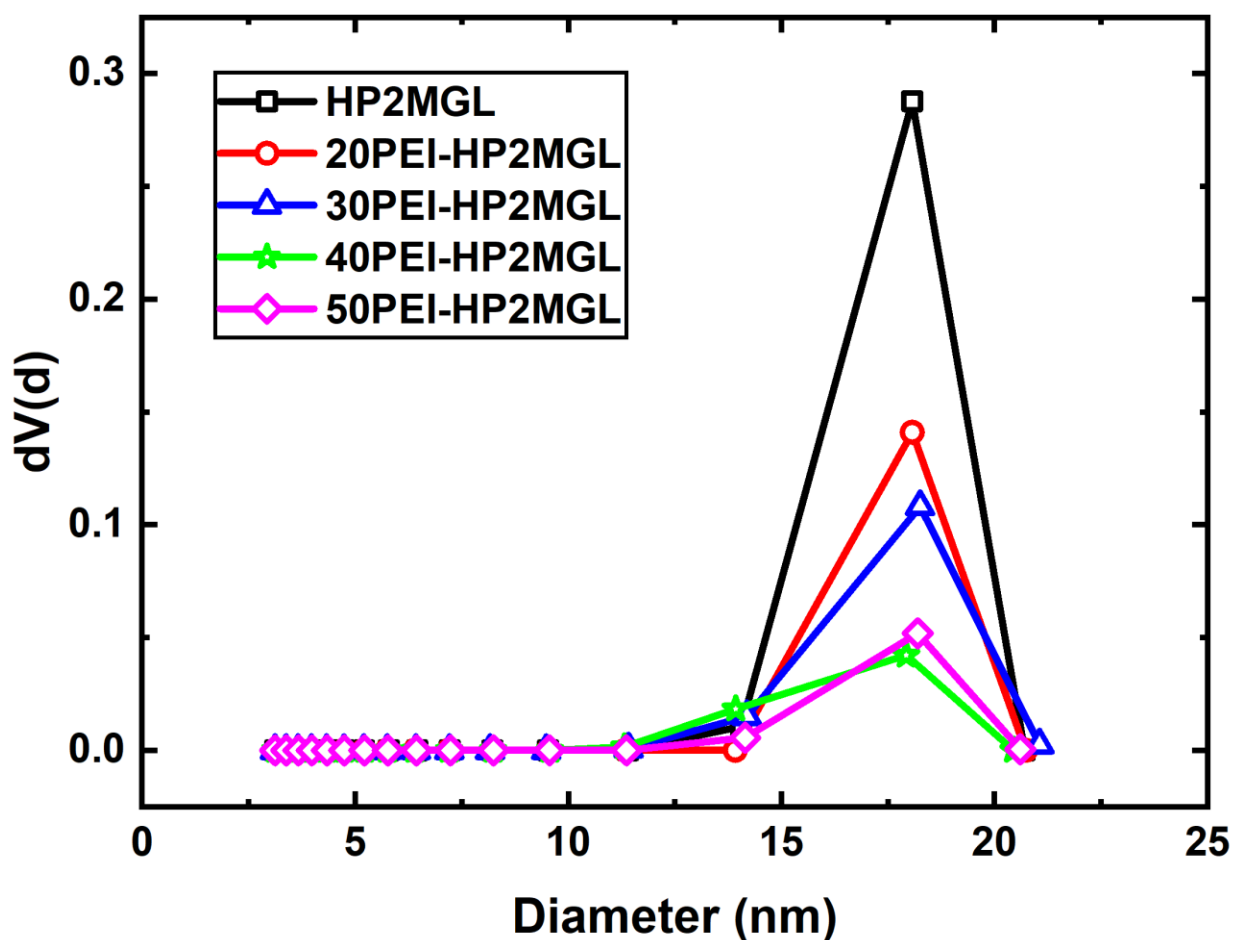


Figure 3.1: Pore size distribution of HP2MGL and xPEI-HP2MGL.

The band center around $3100\text{--}3700\text{ cm}^{-1}$ shifted from 3423 cm^{-1} to 3250 cm^{-1} , representing the NH stretching from PEI atoms in the sorbents.¹²⁷ Also, the peaks at 2955 cm^{-1}

and 2840 cm^{-1} were ascribed to CH_2 vibrations from the PEI molecules.¹²⁸ The 1571 cm^{-1} peak indicates C-N and 1460 cm^{-1} peak accredited to the NH_2 bending vibrations from the PEI.¹²⁸ The sharp and intense peak at 1725 cm^{-1} is attributed to the carbonyl group.¹²⁹ Also, the spectra peaks in the range of $1254\text{--}1134\text{ cm}^{-1}$ represent C-O-C stretching vibration.¹³⁰

Figure 3.3a shows the CO_2 adsorption isotherm of original HP2MGL and at the different amine loading. The CO_2 uptake of the support was the lowest of all samples at all relative pressures. The CO_2 adsorption on pristine HP2MGL, being a macroporous material, is limited to physisorption and is influenced mainly by CO_2 partial pressure. The significant reduction in surface area due to amine loading did not mitigate CO_2 adsorption in PEI-modified resins, indicating that the positive impact on CO_2 adsorption capacity by adding polarizing amine sites surpasses the negative influence due to a smaller surface area.¹³¹ At lower relative pressures, isolated amine sites on the sample begin to adsorb CO_2 molecules by chemical bonding. As gas pressure increases, most of the amine sites are taken, and CO_2 physically adsorbs to form a monolayer. An additional increase in the relative pressure may lead to a multi-layer surface coverage. An incremental rise in the gas pressure will result in complete coverage of the sample and complete pore filling.

The derived CO_2 adsorption capacities of modified resins from the adsorption isotherm by determining the amount of CO_2 molecules chemically adsorbed at zero relative pressure is shown in Figure 3.3b. The $2.7\text{ mmol/g}_{\text{ads}}$ exhibited by 30PEI-HP2MGL represented the highest observed adsorption capacity by the modified resins in the pure CO_2 atmosphere. The increase in the amount of PEI loading results in an initial increase in CO_2 uptake until maximum capacity was observed at 30% loading. Further addition leads to a reduction in CO_2 uptake and which is due to

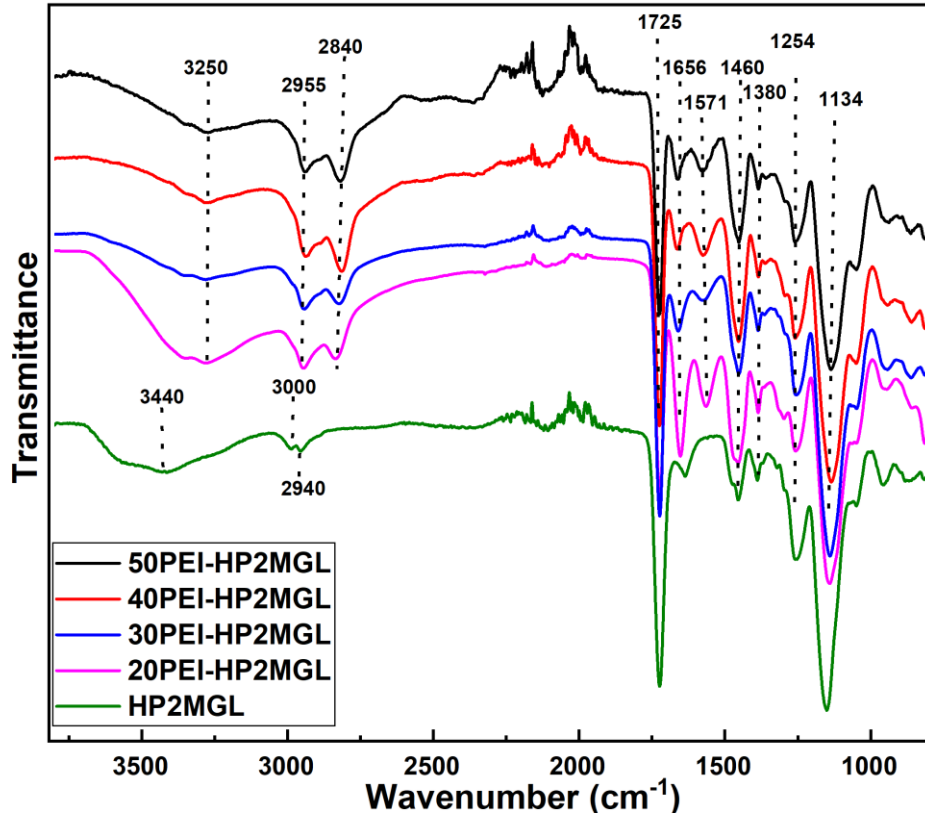


Figure 3.2: FT-IR spectra of different samples

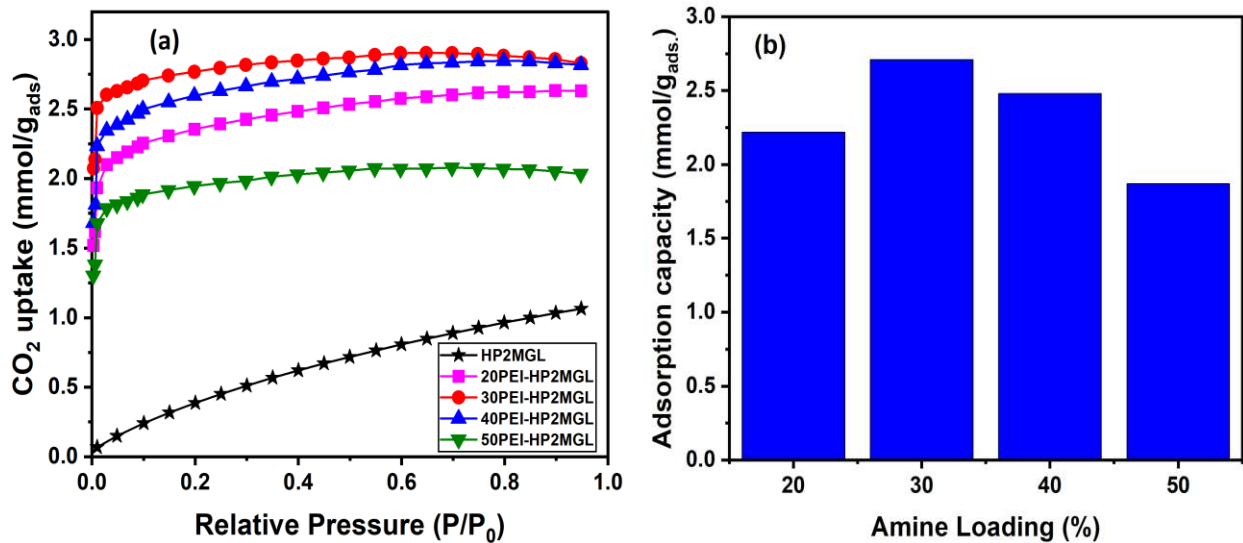


Figure 3.3: (a) CO₂ adsorption isotherm of HP2MGL and xPEI-HP2MGL (b) CO₂ adsorption capacities at different amine loading

the diffusional limitation of CO₂ within the pore of the sorbents. The high concentration of impregnated PEI in the support pores, causing the pore blockage. CO₂ molecules could not access hidden amine sites due to pore blocking, therefore, limiting the amine-CO₂ reaction and which results in lower CO₂ adsorption capacity even at higher amine concentration.

3.2.2 CO₂ Separation Performance of Adsorbents

The impact of methane on the CO₂ adsorption performance of adsorbents was investigated in simulated biogas conditions. The adsorption capacity and breakthrough curve of modified resins in the presence of CH₄ is shown in Figure 3.4. Table 3.2. displays the time it takes to break through the bed and saturated adsorption capacity of different loading of the adsorbents. The saturated adsorption capacity followed the pattern observed from the CO₂ adsorption isotherm pattern shown in figure 3.4. The presence of CH₄ in the feed has neither promoting nor degrading effect on the adsorbent uptake capacity at each amine loading. As observed from Table 3.2, the amount adsorbed at the breakthrough of the adsorbents except in 50PEI-HP2MGL represented for about 85% of the total adsorption capacity, suggesting fast CO₂ kinetics. The 30PEI-HP2MGL has the maximum breakthrough adsorption (2.31 mmol/g_{ads}) and the highest adsorption capacity (2.73 mmol/g_{ads}). Therefore, the 30PEI-HP2MGL was selected for further studies; the influence of water and impurities present in LFG was explored with the sample.

3.2.3 CO₂ Adsorption Performance in Humid Conditions

Moisture is present in LFG at different conditions, which could affect the adsorption of CO₂ in LFG upgrading. The impact of moisture content on CO₂ adsorption was studied by flowing

different amounts of water in addition to CO₂/CH₄ mixture through the 30PEI-HP2MGL sorbents. Figure 3.5 shows the amount of CO₂ adsorbed on 30PEI-HP2MGL in simulated humid biogas conditions increased with increasing moisture content. The CO₂ adsorption capacity increased from 2.73 mmol/g_{ads} in dry simulated biogas conditions by 7% to 2.92 mmol/g_{ads} at 3.8% humid CO₂/CH₄ conditions.

Table 3.2: The breakthrough time and adsorption capacities of 30PEI-HP2MGL

Samples	Breakthrough Time (s)	Breakthrough capacity (mmol/g _{ads})	Saturated capacity (mmol/g _{ads})	Breakthrough /Saturated capacity (%)
20PEI-HP2MGL	280	1.7	2.0	85
30PEI-HP2MGL	330	2.3	2.7	85
40PEI-HP2MGL	300	2.2	2.5	88
50PEI-HP2MGL	260	1.5	1.9	79

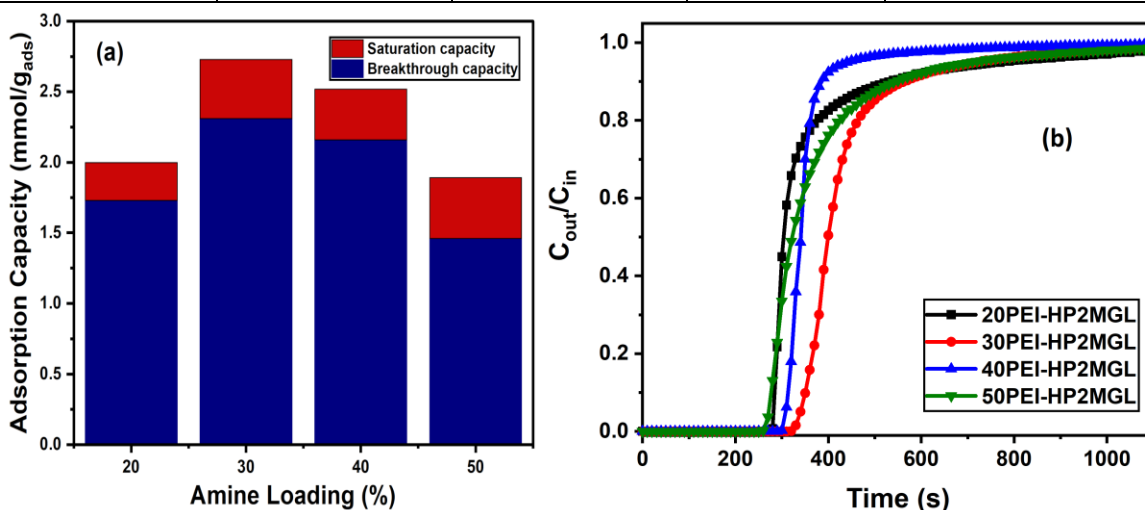


Figure 3.4: (a) CO₂ adsorption capacity of different loading of amine on HP2MGL (b) Breakthrough adsorption curves.

The presence of water promotes the CO₂ adsorption on hydrophobic solid amine adsorbent⁶⁹, such as PEI-modified HP2MGL, because of assisted protonation during the reaction of CO₂ and amine group⁴³. At low moisture content such as typical LFG moisture content, moles of adsorbed CO₂ significantly increased with the vapor content of the feed gas.

3.2.4 Adsorbent Stability Performance

The presence of moisture promotes the adsorption of CO₂ on the adsorbent, but it is essential to test the regenerability of the adsorbent in the humid biogas conditions. The CO₂ adsorption and desorption cycles were performed with 40 sccm of feed flow rate with a 3.8% H₂O composition.

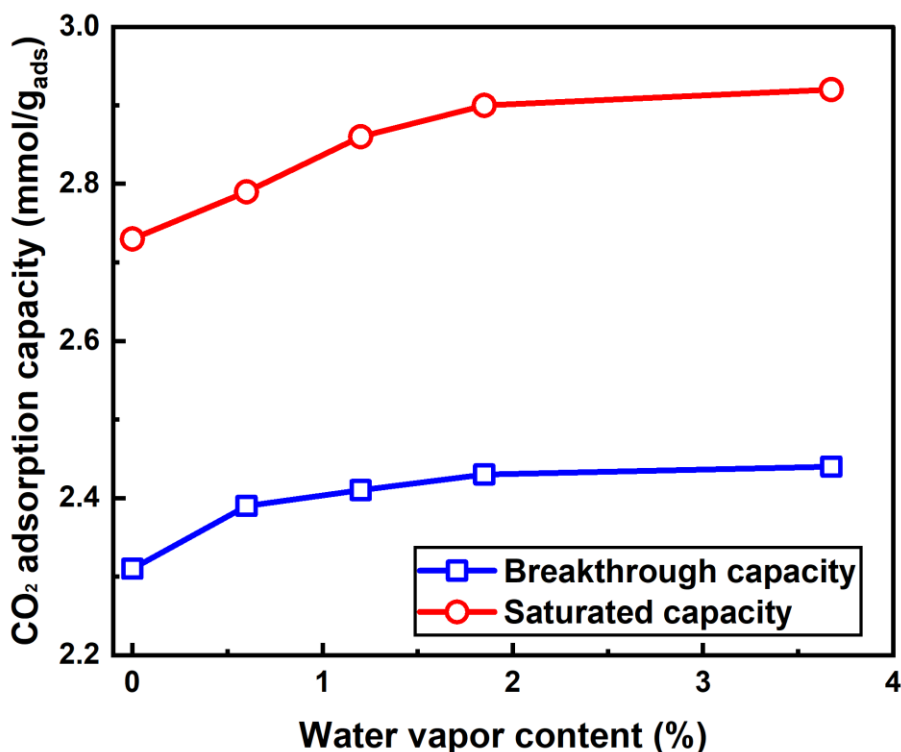


Figure 3.5: CO₂ adsorption capacities of 30PEI-HP2MGL under various moisture conditions

As observed in Figure 3.6, when the adsorption was repeated five times, the saturated CO₂ uptake capacity remained at 2.9 mmol/g, showing both H₂O and CO₂ molecules completely desorbed from the adsorbent at 100 °C.

3.2.5 Adsorption and Desorption Mechanism

The adsorption and desorption characteristics were studied by in-situ CO₂ DRIFTS to understand the reaction mechanism between CO₂ and amine during the CO₂ capture and regeneration phase by the PEI-impregnated resin.

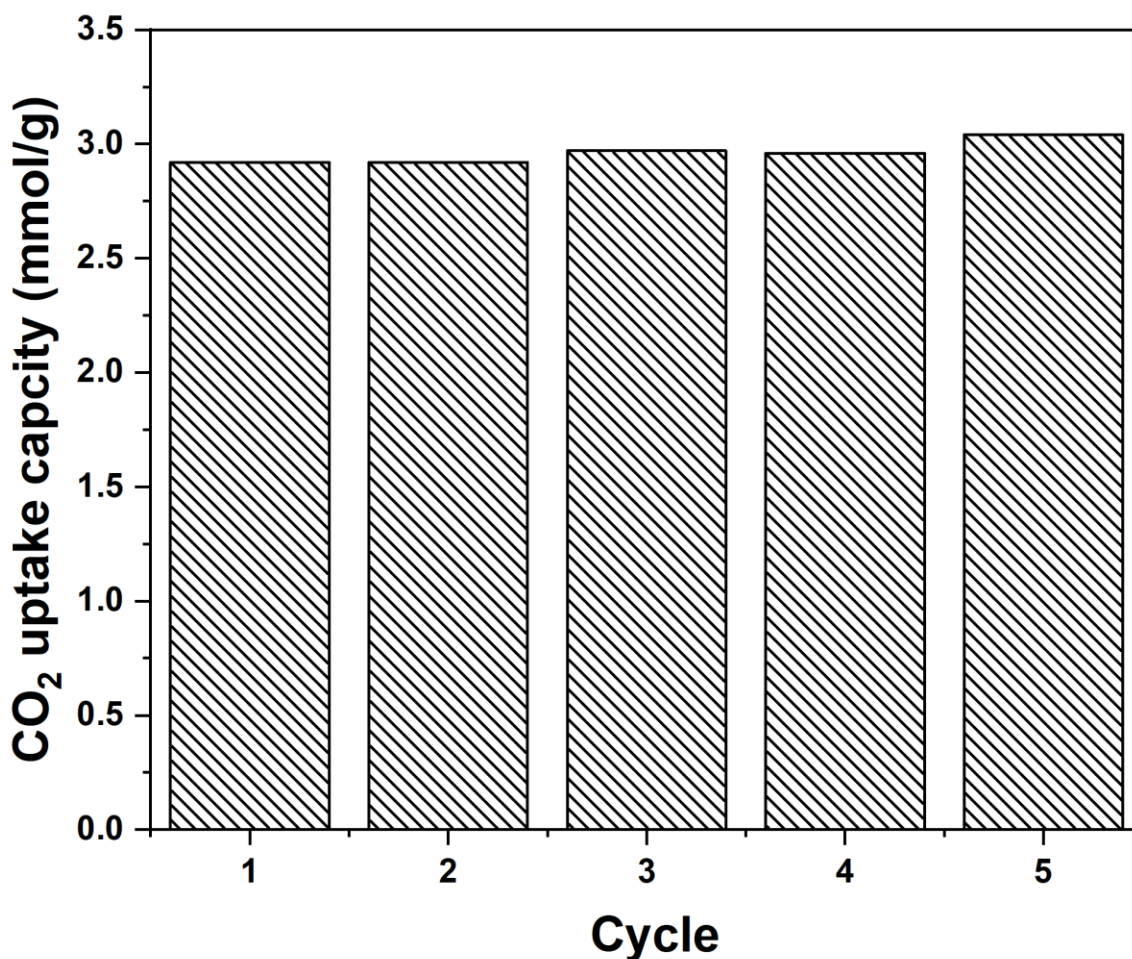


Figure 3.6: CO₂ adsorption capacity of 30PEI-HP2MGL during adsorption-desorption cycles in simulated 3.8%-humid biogas conditions.

An overview of the CO₂ adsorption and desorption cycle mechanism on PEI-HP2MGL sorbent, including CO₂ adsorption and argon purge at 25°C, and temperature-programmed desorption at 100 °C is presented in Figure 3.7. Relevant absorption peak and assigned functional groups are listed in Table 3.3. Figure 3.7 (a) shows the DRIFTS spectra of CO₂ adsorbed on the sorbent with time. The stretching of NH at 2899-3190 cm⁻¹, NH₂⁺, and COO⁻ vibrations at 2360, 2341 cm⁻¹, NH₃⁺ deformation at 1626 cm⁻¹, and N-C stretching at 1412 cm⁻¹ began to appear immediately the reaction starts and gradually increased. The increase in ammonium ion bands (NH₃⁺ and NH₂⁺) intensities and the shifted ammonium-carbamate peaks (NCOO⁻ and NHCOO⁻) shows secondary reactions of adsorbed CO₂ with amines group¹³² as CO₂ flow time increases. CO₂ adsorbed on primary amine sites initially to form primary NH₃⁺ and NHCOO⁻ ion pairs and subsequently to the secondary amine sites for the formation of ammonium ions¹³².

Analysis of the Adsorbed CO₂ spectra and various peak intensity during reaction suggested the adsorption of CO₂ on the PEI-HP2MGL relatable with the zwitterion mechanism.^{35, 132-134} Amine groups (primary or secondary), acting as a base, interact with the acidic CO₂ to form ammonium-carbamate (zwitterion intermediate). Then, the zwitterion intermediate products are deprotonated by free neighboring amine groups to produce ammonium-carbamate ion pairs. The mechanism of CO₂ adsorption is as follows;



Figure 3.7 (b) and (c) show the DRIFTS spectra of adsorbed CO₂ during Argon purge and temperature programmed desorption of amine-impregnated resins, respectively. After CO₂

adsorption, the CO₂ partial pressure was reduced by Argon flow only at 25 °C. Some of the adsorbed CO₂ were desorbed from the sorbent surface, proven by the reduction in peak intensities of ammonium ions and carbamate. The intermediates desorbed at room temperature, and no CO₂ flow was classified as weakly adsorbed CO₂.¹³² Heating of the adsorbent resulted in accelerated desorption of CO₂, cumulated at 100 °C. There are similar DRIFTS spectra during the desorption phase and adsorption phase, supplementary proving the reversibility of CO₂ interactions with the amine sites of the adsorbents. The CO₂ molecules which were desorbed by heating were classified as strongly adsorbed species.¹³²

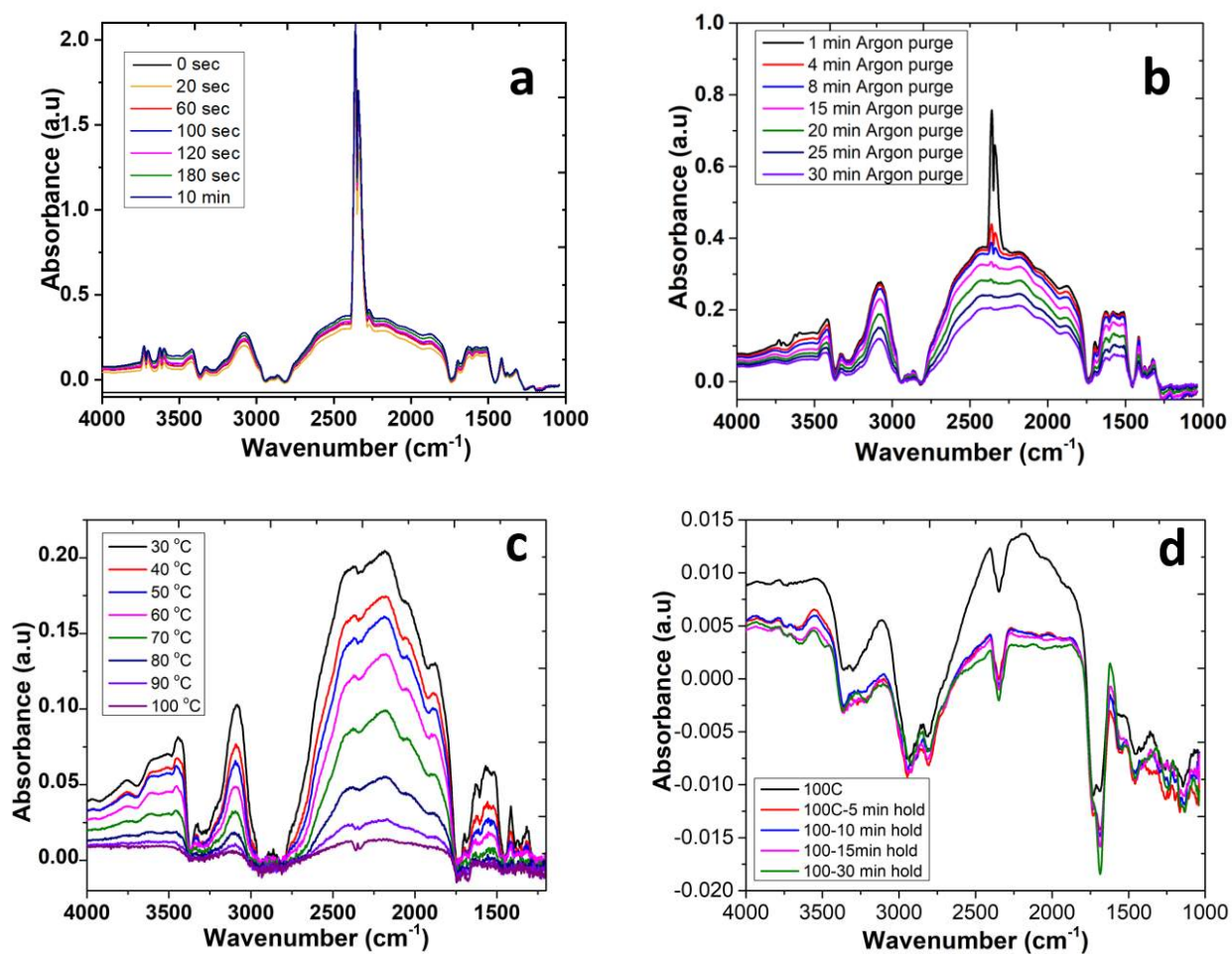


Figure 3.7: The CO₂ in-situ DRIFTS spectra of 30PEI-HP2MGL.

Table 3.3: IR band assignment of PEI-HP2MGL and adsorbed CO₂.^{35, 132-134}

Wavenumber (cm ⁻¹)	Assignment	Species
3420	NH ₂	b-PEI
3329	NH ₂ /NH	b-PEI
3082	NH ₃ ⁺	b-PEI
2899-3190	N-H stretching	Ammonium ions
2861	C-H stretching	b-PEI, HP2MGL
2386-2281	CO ₂ stretching vibration	Gas-phase CO ₂
2360, 2341	NH ₂ , COO ⁻ vibrations	Physiosorbed CO ₂
1695	C=O stretching	Carbamic acid
1626	NH ₃ ⁺ deformation	Primary ammonium ions
1578-1511	COO ⁻ stretching vibration	Carbamate ion
1412	N-C stretching vibration	NHCOO ⁻
1321	NCOO ⁻ skeletal vibration	Carbamate ion

Chapter 4: Techno-Economic Analysis of Biogas Upgrading Units Using Supported Amine Sorbents (SAS)

A preliminary economic analysis of biogas upgrading using the amine-modified silica unit was performed using a simple process design. The main objective was to evaluate the sensitivity of economics to essential process variables. We considered fixed-bed adsorption using steam as the driving force for sorbent regeneration. The reason for the selection of the fixed-bed adsorption system is because of the ease of system operation and lower capital investment. The adsorption system consists of a two-packed bed process vessel system, where one packed bed is in adsorbing CO₂, and the other is regenerated by steam stripping. When the adsorbing packed-bed is saturated with CO₂, the operation of the two packed-beds between adsorption/regeneration modes is switched by a valve. The adsorption cycle begins with the bed packed with sorbents being regenerated until CO₂ is completely desorbed from the sorbent. Then CO₂ from the feed raw biogas will be adsorbed till the packed-sorbent completely saturated and regenerated.

Equipment required for SAS units

1. Process Vessel
2. Compressor/blower
3. Pipes and Valve

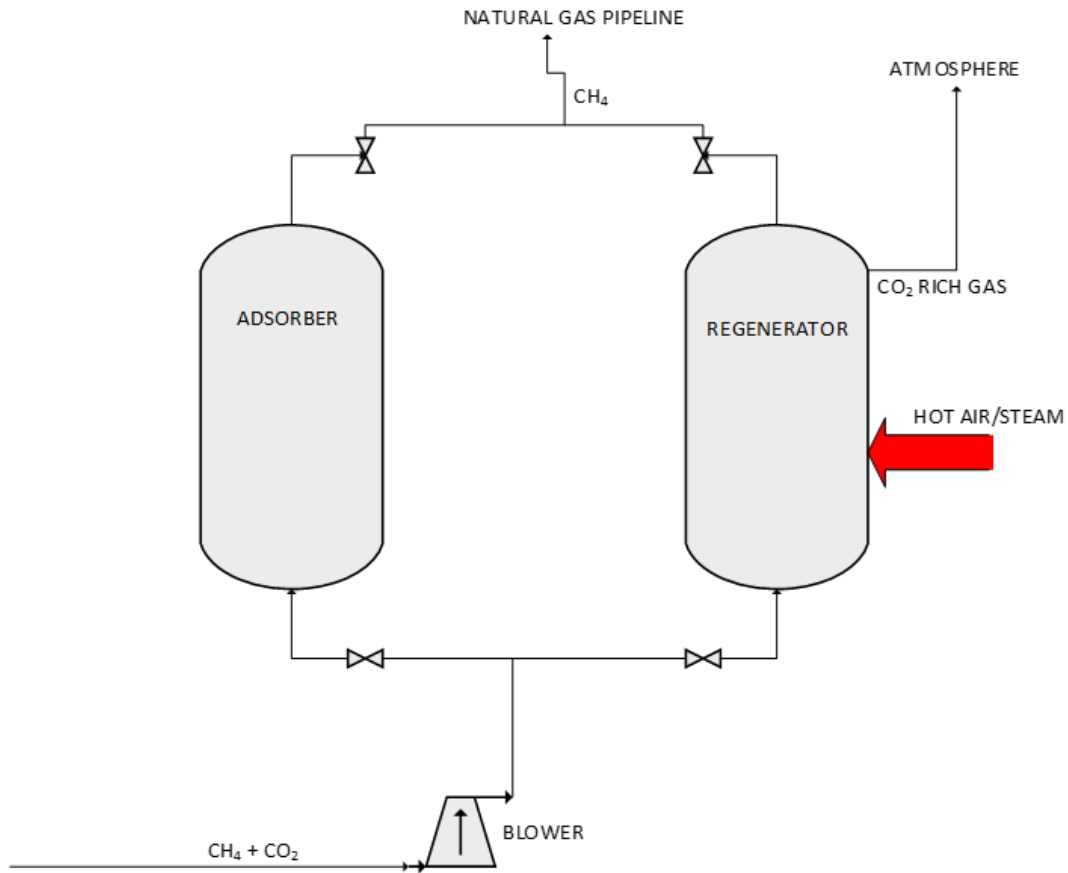


Figure 4.1: An illustrative process model for a SAS unit for CO₂ separation from biogas.

4.1 Typical SAS Units Design Conditions

The following basis and assumption were used to simulate the Supported Amine Sorbent (SAS) unit process performance:

- The process design conditions used are shown in Table 4.1. The feed composition is the average of a typical biogas composition (35%-45% CO₂, 55%-65% CH₄) after the removal of impurities. The feed pressure and temperature of a typical biogas plant are atmospheric pressure and room temperature, respectively. ¹³⁵

- The product purity is based on the natural gas grid guideline ¹³⁶. Methane losses at biogas upgrading plants are typically about 1.5% of upgraded biogas ¹³⁷.
- The height to diameter ratio of the adsorbing vessel is assumed as 10 to reduce pressure loss across the column and increase the contact area between the biogas and the adsorbent.
- The sorbent was regenerated at 100 °C¹³⁸. The sorbent's longevity is assumed as six-month (2000 regeneration cycles).

4.2 Equations Used

$$\text{Mass of adsorbent} = \frac{\text{Mass of adsorbate (kg}_{\text{CO}_2})}{\text{Adsorption Capacity (}\frac{\text{kg}_{\text{CO}_2}}{\text{kg}_{\text{ads}}})}$$

$$\text{Mass of adsorbate} = m_{\text{CO}_2}$$

$$= \text{Volumetric flowrate} * \text{Adsorbate density} * \text{Ratio of components} \\ * \text{Adsorption time}$$

$$\text{Volume of sorbent required} = \frac{\text{Required mass of sorbent (kg)}}{\text{Adsorbent density (kg/m}^3)}$$

$$\text{Volume of process vessel required} = (1 + \text{bed void volume}) * \text{Volume of adsorbent required}$$

4.3 Economic Model

4.3.1 Capital Cost/Fixed Capital Investment (FCI) Estimation

The fixed capital investment is the summation of the costs of major plant equipment and installation cost.

Table 4.1: SAS design conditions

Feed composition	60% CH ₄ , 40% CO ₂
Maximum feed flowrate, SCFM	2500 ¹³⁹
CH ₄ purity in product	98%
CH ₄ loss	1.5%
Feed Pressure, bar	1
Feed Temperature, °C	25
Regeneration Temperature, °C	100
Source of heat for regeneration	Steam
Bed void volume	45% ¹³⁹
Number of adsorbers	2
Adsorption time, hours	2
Process vessel (Height to Diameter ratio)	10
Adsorbent density, kg/m ³	200.5 (APTES-SBA15), 1090 (PEI-HP2MGL)
Adsorbate density, kg/m ³	1.977 ¹⁴⁰
Adsorbent heat capacity, J/kg.K	920 (APTES-SBA15) ¹⁴¹ , 1466 (PEI-HP2MGL)
Adsorption capacity, mmol _{CO2} /g _{ads}	0.85 (APTES-SBA15), 2.7 (PEI-HP2MGL)
Regeneration capacity, cycles	2000

The major equipment required, as shown in figure 4.1, includes two process vessels (adsorbers) and a compressor or blower to overcome pressure loss in the adsorbing column. The cost estimation of the vertical process vessel and compressor is based on volume capacity and fluid power, respectively, as in published correlations (Eqn A.1 and Eqn A.2) ¹⁴². The total capital cost calculated is distributed over ten years and annualized in the operating cost of the plant.

Table 4.2: Eqn A.1 equipment costing data ¹⁴²

Equipment type	Equipment Description	K ₁	K ₂	K ₃	Capacity, A, units
Process Vessel	Vertical	3.4974	0.4485	0.1074	Volume, m ³
Pump	Reciprocating	3.8696	0.3161	0.1200	Shaft Power, kW
Compressor	Centrifugal	2.2891	1.3604	-0.1027	Fluid Power, kW

$$C_p = \text{Capital cost} = \text{Antilog}_{10}(k_1 + k_2 \log_{10} A + k_3 (\log_{10} A)^2) \quad \text{---Eqn A.1}$$

Pressure factor

$$F_{p,vessel} = \text{Pressure factor} = \frac{\frac{(P + 1)D}{2(850 - 0.6(P + 1))} + 0.00315}{0.0063}$$

Where D= diameter of the vessel in meters, and P= Operating pressure (barg)

Material Factor and Bare module

$$C_{bm} = \text{Bare Module cost} = C_p F_{bm} = C_p (B_1 + B_2 F_m F_p) \quad \text{---Eqn A.2}$$

Table 4.3: Eqn A.2 bare Module Factor Constants

Equipment	Equipment material	Material factor, F_m	B_1	B_2
Process Vessel	Carbon steel	1.0	2.25	1.82

4.3.2 Operating Cost Calculations

- I. Fixed Capital Investment (FCI)
- II. Cost of utilities (C_{UT})
- III. Cost of operating Labor (C_{OL})
- IV. Cost of Raw materials (C_{RM})
- V. Cost of waste treatment (C_{WT})

$$\text{Operating Cost} = C_{RM} + C_{WT} + C_{OL} + 0.1FCI + C_{UT} \text{ ---Eqn A.3}$$

a. Cost of operating labor

An operator is expected to works average 49 weeks/year and five 8-hour shifts/week. [49 weeks/year * 5 shifts/week] = 245 shifts per operator per year.

This requires (365 days/year * 3 shifts/day) = 1095 operating shifts per year / (245 shifts/operator/year) = 4.5 operators are hired for each operation needed in the plant at any time.

Plant and system operator wage = \$26.48/hr. ¹⁴²

$$N_{oi} = (6.29 + 31.7P^2 + 0.23N_{op})^{0.25}$$

N_{oi} = Number of operators per shift

P = Number of processing steps involving the handling of particulate solids

N_{op} = Number of non-particulate processing steps

In this case study, there are no particulate solids processing units, and only the adsorber is considered for non-particulate processing equipment.

$N_{op} = 1$

$$N_{oi} = (6.29 + 31.70^2 + 0.23 * 1)^{0.25}$$

$$N_{oi} = 1.597$$

Operating Labor = Number of operators hired per operation * Number of operators per shift, N_{oi}

$$\text{Operating Labor} = 4.5 * 1.597 = 7.16 \approx 7$$

$$\text{Labor Cost} = \text{Operating Labor} * \text{Wage} * 2000(\text{hour/year}) = 7 * 26.48 * 2000 = \$370,720 \text{ per year}$$

b. Cost of utility/regeneration cost

$$\text{Cost of steam from boiler (Low pressure (5 barg, } 160^{\circ}\text{C))} = \$13.28/\text{GJ}^{142}$$

$$\text{Energy required for regeneration} = (\text{Mass of adsorbent} * \text{Specific heat capacity} * \text{Temperature}) /$$

Heating efficiency

Where Heating Efficiency = 50%

c. Cost of raw materials

1. 3-Aminopropyltriethoxysilane APTES = \$5.0 per kg ¹⁴³
2. SBA-15 = \$1,690 per 1000 kg¹⁴³
3. HP2MGL = \$7.34 per kg ¹⁴³
4. PEI = \$1 per kg¹⁴³

4.4 Excel Model Outlook

Row	Parameter	Value	Unit
2	Volumetric Flowrate	2500	SCFM
3		4285.713	Nm ³ /hr
4	Adsorption Capacity	2.7	mmol/g
5	Regeneration Capacity	2000	Cycle
6	Mass of adsorbent required	55345	Kg
7	Adsorbent Cost	\$ 56,000.00	
8		\$ 1.01	per Kg
9	Volume of Process Vessel	79.5338159	m ³
10			
11	Process Vessel Height	21.632	m
12	Process Vessel Diameter	2.163	m
13	Operating Pressure	1	bar
14	Compressor Capacity	10	kW
15	Vessel Purchase Cost	\$ 55,000	per unit
16	Vessel Bare Module Cost	\$ 214,000	per unit
17			
18	Compressor Purchase Cost	\$ 4,000	per unit
19	Compressor Bare Module Cost	\$ 10,000.00	per unit
20			
21			
22	Adsorption temperature	25	Degree
23	Regeneration Temperature	100	Degree
24	Steam unit cost	13.28	\$/GJ
25	Energy Required	12.2	GJ

Figure 4.2: Excel data input tab

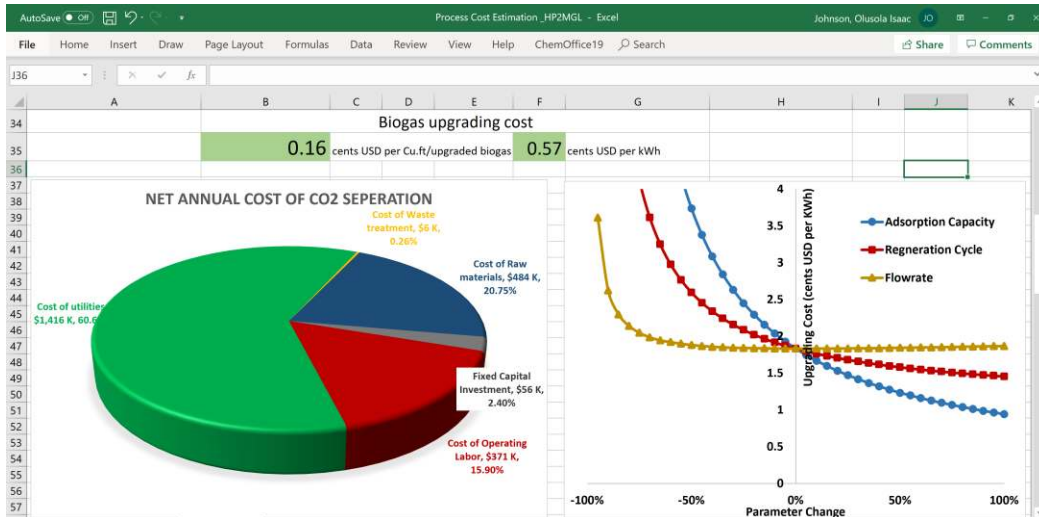


Figure 4.3: Excel result tab

4.5 Results and Discussion

The economic calculations of biogas upgrading using Supported Amine Sorbent (SAS) were performed. Two adsorbing columns of capacity, 530 m³, and packing height, 40m was estimated for APTES-SBA15 compared to volume capacity, 80 m³, and packing height, 22m in PEI-HP2MGL. The capital cost was estimated to be 9.5 and 0.5 million USD, respectively, for APTES-SBA15 and PEI-HP2MGL, respectively, as summarized in Table 4.4. The annual cost of upgrading is approximately is 7.9 million USD using APTES and reduced significantly to 2.4 million USD in PEI-HP2MGL, distributed across the cost of raw materials, and the cost of utilities or regeneration costs as 41 and 37%, respectively in APTES-SBA15, as shown in Figure 4.3(a). In the PEI-HP2MGL utilization, the cost of utilities associated with the regeneration of sorbents accounts for more than 65% of the biogas upgrading cost, as presented in Figure 4.3 (b). The SAS is an improvement compared with other technology such as amine scrubbing with high regeneration energy consumption.

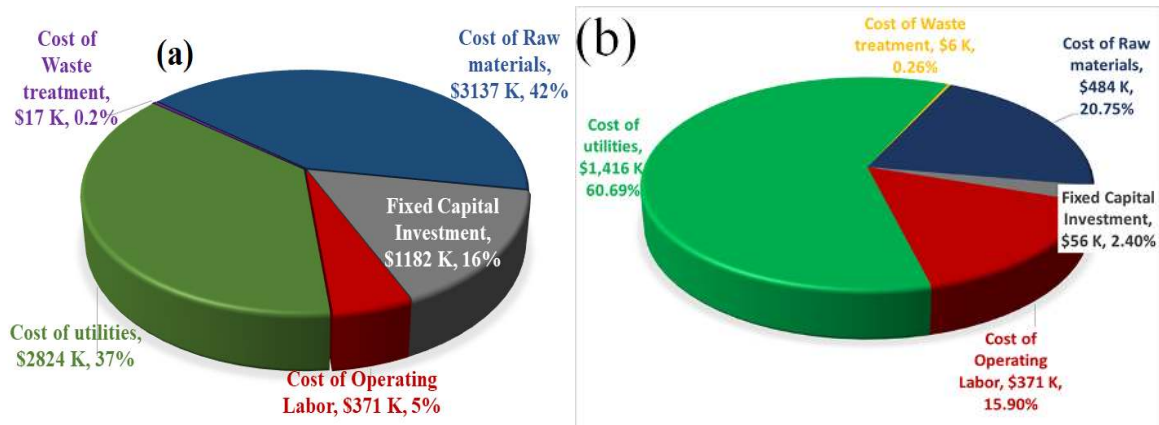


Figure 4.4: Biogas annual upgrading cost breakdown (a) APTES-SBA15 (b) PEI-HP2GML

4.5.1 Sensitivity Analysis

The biogas upgrading cost was subjected to sensitivity studies to study the effect of the plant design parameter and sorbent properties. The critical parameter considered are adsorption capacity, regeneration cycles, and plant capacity, which could potentially affect the economic viability of the amine-modified silica unit. The sensitivity analysis results were shown in figure 4.5. The cost of CO₂ separation from biogas using amine-modified silica is most sensitive to the adsorption capacity.

4.5.2 Comparison with Existing Technologies

The capital cost data obtained from the design project is compared with other existing technologies and for all capacities of plant considered. The amine-modified sorbent units have the lowest fixed capital investment, as shown in Figure 4.6. The current biogas upgrading technologies considered include high-pressure water scrubbing (HPWS), pressure swing adsorption (PSA), membrane separation, and chemical scrubbing Process (CSP).²⁴ The capital cost per plant capacity (m³/hr.) decreased with the increasing size until the plant capacity of 600 m³/hr., as it increases with increasing plant capacity in the SAS units utilizing APTES-SBA15.

The economy vs. the scale of plants for the different upgrading techniques and sizes of the upgrading plant was shown in figure 4.7. All for the processes considered, the cost decreases with the increasing biogas plant capacity. The amine-modified resin unit has the lowest cost of upgrading per kWh of bio-methane at all plant capacities.

Table 4.4: SAS Capital Cost (2019)

Equipment	Purchase Cost per unit (kUSD)		Bare Module Cost per unit (kUSD)		Total cost (kUSD)	
	APTES- SBA15	PEI- HP2MGL	APTES- SBA15	PEI- HP2MGL	APTES- SBA15	PEI- HP2MGL
Process Vessels	\$ 872	\$ 55	\$ 4,715	\$ 214	\$ 9,430	\$ 428
Blower	\$ 4 ⁴⁹	\$ 4 ⁴⁹	\$ 10	\$ 10	\$ 20	\$ 20
Capital Cost					\$ 9,450	\$ 448

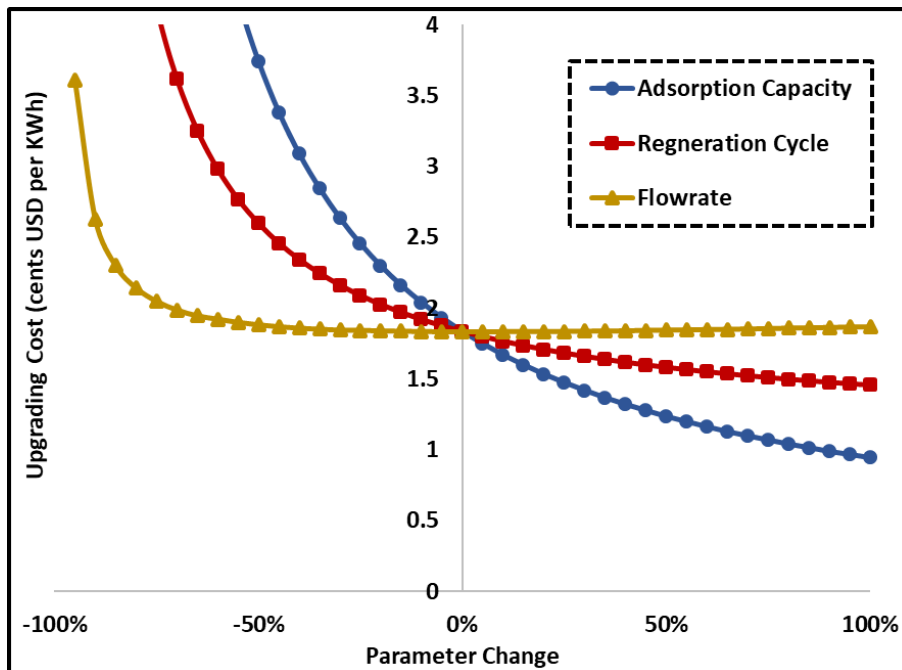


Figure 4.5: Sensitivity results. The base case is based on 0.85 mmol_{CO2}/gads adsorption capacity, 2000 SCFM flow rate, and 2000 regeneration cycles allowed for the adsorbent.

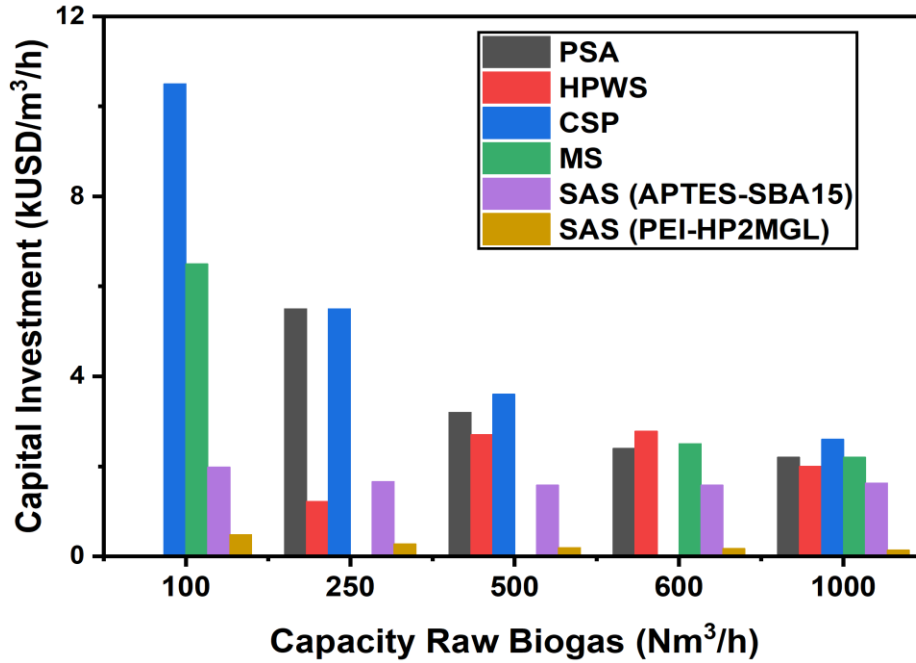


Figure 4.6: Capital investment cost of different upgrading technologies. (non-SAS data ⁵¹)

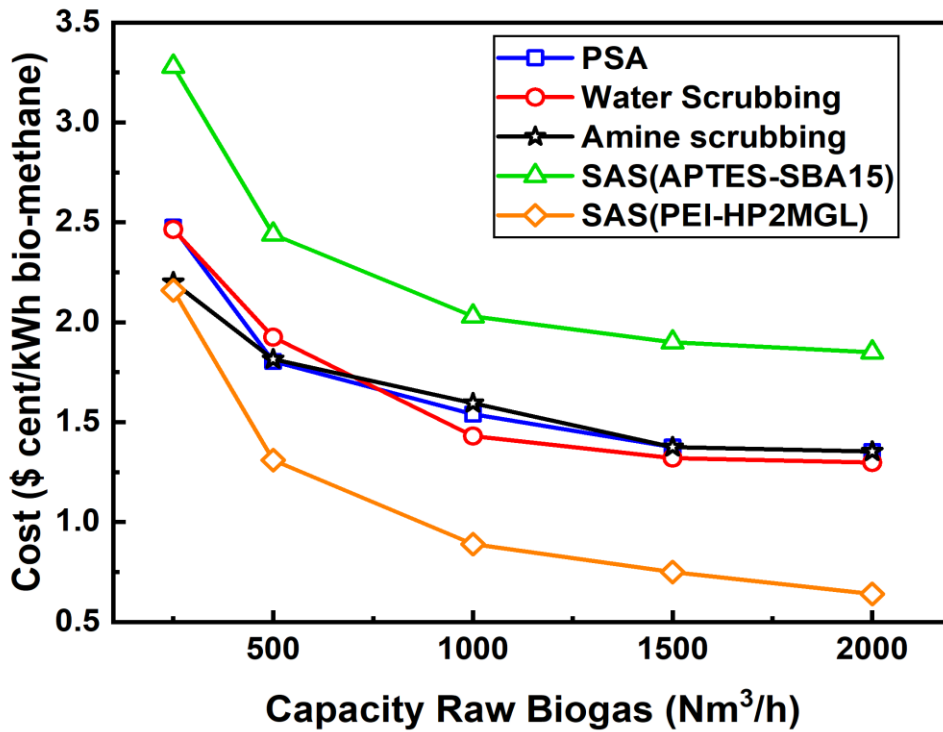


Figure 4.7: Cost for biogas upgrading for methane (PSA, water scrubbing, and amine scrubbing data). ⁵²

4.5.3 Comparison to Natural Gas

Natural gas market value averaged at \$3.48 per 1000 cubic feet of natural gas from October 2018 to September 2019, ranging from \$ 4.93 to \$ 2.03 per 1000 cubic feet of natural gas¹⁴⁴. The current price pegged at \$2.25 per 1000 ft³ of natural gas. The cost of bio-methane produced from this technology when APTES SBA15 is used is \$5.2 per 1000 cubic feet of bio-methane from the economic calculations. However, at using PEI-HP2MGL at the same conditions, the price is estimated to reduce drastically to \$1.6 per 1000 cubic feet of bio-methane. The Bio-methane price from the utilization of PEI-HP2MGL will currently compete with natural gas even without renewable energy credit. Improvements in adsorptive CO₂ technology and the access to government renewable energy credit will further promote the usage and economic viability of renewable natural gas generated from this technology.

Chapter 5: Summary, Conclusions, and Recommendations

In this study, the application of a PEI-impregnated HP2MGL adsorbent synthesized for carbon dioxide separation from biogas was evaluated. Through material characterization, PEI was successfully loaded into the pores of resin supports through the wet-impregnation method, and the sorbent at 30% amine loading exhibits the highest adsorption capacity. Also, experiments to study separation performance, regeneration, sorbent stability, and simulated biogas were carried out in a fixed bed system at room temperature.

PEI-modified resin sorbent exhibited an excellent adsorption capacity $2.7 \text{ mmol}_{\text{CO}_2}/\text{g}$ in pure CO_2 and simulated CH_4/CO_2 mixtures, with negligible CH_4 adsorbed at room temperature. The sorbent adsorption capacity increased to $2.92 \text{ mmol}_{\text{CO}_2}/\text{g}_{\text{ads}}$ in humid conditions, proving the promoting effect of water vapor on CO_2 uptake. In the presence of water, the adsorbent could be entirely regenerated at 100°C and remains stable over five cycles of adsorption-desorption, proving the sorbent could is stable.

In-situ CO_2 DRIFTS examined the reaction of CO_2 with PEI-impregnated resin. Based on the analysis of the functional groups' spectra band intensities during the adsorption phase, CO_2 adsorbed on the PEI-HP2MGL to form ammonium-carbamate, consistent with the zwitterion mechanism. Desorption of adsorbed CO_2 species from amine-impregnated resin occurs by the removal of weakly adsorbed species by reduction of CO_2 partial pressure and by removal of the ammonium-carbamate ions through increasing of temperature to 100°C for desorption of

strongly bonded CO₂ molecules. The process economic studies evaluated the potential of the Supported Amine Sorbent adsorptive CO₂ separation system for biogas upgrading. Supported Amine Sorbent (SAS) technology provides the technical capacity to satisfy the requirement of gas quality. It also provides a reduction in energy consumption in addition to cost minimization.

The sensitivity study of the process determined the process economics is primarily dependent on plant capacity, allowed regeneration cycles, and adsorption capacity of the adsorbent used. The adsorbent's cyclic stability is the most important property as it controls the lifespan of the material. The PEI-modified sorbent with the adsorption capacity of 2.7 mmol_{CO₂}/g_{ads} and regenerability of 2000 cycles achieve economic viability with natural gas. In comparison to other biogas upgrading technologies, SAS is projected to require the least fixed capital investment in comparison with chemical scrubbing, membrane separation, water scrubbing, and Pressure Swing Adsorption. The cost of upgrading per kWh of bio-methane of the Supported Amine Sorbent decreases with the increasing capacity of the biogas plant. It also recorded the lowest price of upgrading at all plant capacity compared with other upgrading technologies.

The commercial utilization of separated CO₂ can further improve the economic viability of biogas upgrading via a supported amine system. Captured carbon dioxide can be commercialized for other end-uses, like algae production, enhanced oil recovery (EOR), and mineralization. The development of sorbent with higher adsorption capacity and lower regeneration temperature should be explored. A detailed study on long term exposure of CO₂ on sorbents and their cyclic stability of over more extended periods of adsorption-desorption cycles (possibly thousands of cycles) should be considered.

References

1. PBL Netherlands Environmental Assessment Agency; Trends in Global CO₂ emissions: 2016 Report <https://www.pbl.nl/en/publications/trends-in-global-co2-emissions-2016-report> (accessed 04/18/2020).
2. Stern Review: The Economics of Climate Change https://www.brown.edu/Departments/Economics/Faculty/Matthew_Turner/ec1340/readings/Sternreview_full.pdf (accessed 4/18/2020).
3. U.S. Energy Information Administration - EIA - Independent Statistics and Analysis; EIA projects nearly 50% increase in world energy usage by 2050, led by growth in Asia - Today in Energy - U.S. Energy Information Administration (EIA). <https://www.eia.gov/todayinenergy/detail.php?id=41433#> (accessed 04/18/2020).
4. Annan, J. D.; Hargreaves, J. C., Using multiple observationally-based constraints to estimate climate sensitivity. *Geophysical Research Letters* **2006**, *33* (6).
5. Global Monitoring Laboratory - Global Greenhouse Gas Reference Network; Earth System Research Laboratory; US Department of Commerce. <https://www.esrl.noaa.gov/gmd/ccgg/trends/data.html> (accessed 04/18/2020).
6. change, N. G. c. Global temperature. <https://climate.nasa.gov/vital-signs/global-temperature/> (accessed 04/18/2020).
7. Brohan, P.; Kennedy, J. J.; Harris, I.; Tett, S. F.; Jones, P. D., Uncertainty estimates in regional and global observed temperature changes: A new data set from 1850. *Journal of Geophysical Research: Atmospheres* **2006**, *111* (D12).
8. United Nations Framework Convention on Climate Change (UNFCCC). <http://unfccc.int/resource/docs/2015/cop21/eng/l09r01.pdf>.
9. EPA, U. Municipal Solid Waste. <https://archive.epa.gov/epawaste/nonhaz/municipal/web/html/>.
10. EPA Greenhouse gas emissions. <https://www.epa.gov/ghgemissions/sources-greenhouse-gas-emissions>.
11. Tubiello, F.; Salvatore, M.; Córdor Golec, R.; Ferrara, A.; Rossi, S.; Biancalani, R.; Federici, S.; Jacobs, H.; Flammini, A., Agriculture, forestry and other land use emissions by sources and removals by sinks. *Rome, Italy* **2014**.
12. US Energy Information Administration: Emissions of greenhouse gases in the U. S. https://www.eia.gov/environment/emissions/ghg_report/ghg_methane.php.
13. Persson, M.; Jönsson, O.; Wellinger, A. In *Biogas upgrading to vehicle fuel standards and grid injection*, IEA Bioenergy task, 2006; pp 1-34.
14. Ryckebosch, E.; Drouillon, M.; Vervaeren, H., Techniques for transformation of biogas to biomethane. *Biomass and bioenergy* **2011**, *35* (5), 1633-1645.
15. EPA, U., Inventory of U.S. Greenhouse Gas Emissions and sinks: (1990-2015). **2006**.
16. IPCC Summary for Policymakers of IPCC Special Report on Global Warming of 1.5°C approved by governments. <https://www.ipcc.ch/2018/10/08/summary-for-policymakers-of-ipcc-special-report-on-global-warming-of-1-5c-approved-by-governments/> (accessed 04/18/2020).

17. Bauer, F.; Persson, T.; Hulteberg, C.; Tamm, D., Biogas upgrading–technology overview, comparison and perspectives for the future. *Biofuels, Bioproducts and Biorefining* **2013**, 7 (5), 499-511.
18. Ullah Khan, I.; Hafiz Dzarfan Othman, M.; Hashim, H.; Matsuura, T.; Ismail, A. F.; Rezaei-DashtArzhandi, M.; Wan Azelee, I., Biogas as a renewable energy fuel – A review of biogas upgrading, utilisation and storage. *Energy Convers Manage* **2017**, 150, 277-294.
19. The World Bank; A Global Snapshot of Solid Waste Management to 2050. https://datatopics.worldbank.org/what-a-waste/trends_in_solid_waste_management.html (accessed 03/04/2020).
20. Energy Technology Perspectives 2016; International Energy Agency;. https://www.iea.org/publications/freepublications/publication/EnergyTechnologyPerspectives2016_ExecutiveSummary_EnglishVersion.pdf (accessed 0/19/2020).
21. Jahandar Lashaki, M.; Khiavi, S.; Sayari, A., Stability of amine-functionalized CO₂ adsorbents: a multifaceted puzzle. *Chemical Society Reviews* **2019**, 48 (12), 3320-3405.
22. Awe, O. W.; Zhao, Y. Q.; Nzihou, A.; Minh, D. P.; Lyczko, N., A Review of Biogas Utilisation, Purification and Upgrading Technologies. *Waste Biomass Valori* **2017**, 8 (2), 267-283.
23. Munoz, R.; Meier, L.; Diaz, I.; Jeison, D., A review on the state-of-the-art of physical/chemical and biological technologies for biogas upgrading. *Rev Environ Sci Bio* **2015**, 14 (4), 727-759.
24. Petersson, A.; Wellinger, A. Biogas upgrading technologies-Developments and innovations 2009. http://www.ieabiogas.net/download/publi-task37/upgrading_rz_low_final.pdf (accessed 05.03.2012).
25. Sun, Q.; Li, H.; Yan, J.; Liu, L.; Yu, Z.; Yu, X., Selection of appropriate biogas upgrading technology- a review of biogas cleaning, upgrading and utilisation. *Renewable and Sustainable Energy Reviews* **2015**, 51, 521-532.
26. Thrän, D.; Billig, E.; Persson, T.; Svensson, M.; Daniel-Gromke, J.; Ponitka, J.; Seiffert, M., *Biomethane: Status and Factors Affecting Market Development and Trade: a Joint Study*. IEA Bioenergy: 2014.
27. Sinnott, R.; Towler, G. P., *Chemical engineering design: principles, practice and economics of plant and process design*. Butterworth-Heinemann: 2013.
28. Tock, L.; Gassner, M.; Maréchal, F., Thermochemical production of liquid fuels from biomass: Thermo-economic modeling, process design and process integration analysis. *Biomass and Bioenergy* **2010**, 34 (12), 1838-1854.
29. Lasocki, J.; Kołodziejczyk, K.; Matuszewska, A., Laboratory-scale investigation of biogas treatment by removal of hydrogen sulfide and carbon dioxide. *Polish Journal of Environmental Studies* **2015**, 24 (3), 1427-1434.
30. Deng, L.; Hägg, M.-B., Techno-economic evaluation of biogas upgrading process using CO₂ facilitated transport membrane. *International Journal of Greenhouse Gas Control* **2010**, 4 (4), 638-646.
31. Bauer, F.; Hulteberg, C.; Persson Tobias, D. T., Biogas upgrading-REVIEW of commercial technologies (biogasupppgradering-Granskning av kommersiella tekniker. *SGC rapport* **2013**, 270, 83.
32. Patterson, T.; Esteves, S.; Dinsdale, R.; Guwy, A., An evaluation of the policy and techno-economic factors affecting the potential for biogas upgrading for transport fuel use in the UK. *Energy Policy* **2011**, 39 (3), 1806-1816.
33. Beil, M. In *Overview on biogas upgrading technologies*, European Biomethane Fuel Conference, Goteborg, Sweden, Biogasmax, 2009.
34. Wu, S.-H.; Mou, C.-Y.; Lin, H.-P., Synthesis of mesoporous silica nanoparticles. *Chemical Society Reviews* **2013**, 42 (9), 3862-3875.
35. Chang, A. C.; Chuang, S. S.; Gray, M.; Soong, Y., In-situ infrared study of CO₂ adsorption on SBA-15 grafted with γ -(aminopropyl) triethoxysilane. *Energy & Fuels* **2003**, 17 (2), 468-473.
36. Bagshow, S.; Prouzet, E., Science 269 different pore diameters supporting their assumed (1995) 1242. structure.[8] SA Bagshow, TJ Pinnavaia. *Angew. Chem. Int. Ed. Engl* **1996**, 35, 1102.

37. Gelles, T.; Lawson, S.; Rownaghi, A. A.; Rezaei, F., Recent advances in development of amine functionalized adsorbents for CO₂ capture. *Adsorption* **2020**, *26* (1), 5-50.
38. Chen, C.; Ahn, W.-S., CO₂ capture using mesoporous alumina prepared by a sol-gel process. *Chemical Engineering Journal* **2011**, *166* (2), 646-651.
39. Sakwa-Novak, M. A.; Jones, C. W., Steam Induced Structural Changes of a Poly(ethylenimine) Impregnated γ -Alumina Sorbent for CO₂ Extraction from Ambient Air. *ACS Applied Materials & Interfaces* **2014**, *6* (12), 9245-9255.
40. Castellazzi, P.; Notaro, M.; Busca, G.; Finocchio, E., CO₂ capture by functionalized alumina sorbents: DiEthanolAmine on γ -alumina. *Micropor Mesopor Mat* **2016**, *226*, 444-453.
41. Pokhrel, J.; Bhorja, N.; Anastasiou, S.; Tsooufis, T.; Gournis, D.; Romanos, G.; Karanikolos, G. N., CO₂ adsorption behavior of amine-functionalized ZIF-8, graphene oxide, and ZIF-8/graphene oxide composites under dry and wet conditions. *Micropor Mesopor Mat* **2018**, *267*, 53-67.
42. Liu, Z.-l.; Teng, Y.; Zhang, K.; Cao, Y.; Pan, W.-p., CO₂ adsorption properties and thermal stability of different amine-impregnated MCM-41 materials. *Journal of Fuel Chemistry and Technology* **2013**, *41* (4), 469-475.
43. Xu, X.; Song, C.; Miller, B. G.; Scaroni, A. W., Influence of moisture on CO₂ separation from gas mixture by a nanoporous adsorbent based on polyethylenimine-modified molecular sieve MCM-41. *Industrial & engineering chemistry research* **2005**, *44* (21), 8113-8119.
44. Son, W.-J.; Choi, J.-S.; Ahn, W.-S., Adsorptive removal of carbon dioxide using polyethyleneimine-loaded mesoporous silica materials. *Micropor Mesopor Mat* **2008**, *113* (1), 31-40.
45. Sanz, R.; Calleja, G.; Arencibia, A.; Sanz-Pérez, E., CO₂ adsorption on branched polyethyleneimine-impregnated mesoporous silica SBA-15. *Applied Surface Science* **2010**, *256* (17), 5323-5328.
46. Zhao, A.; Samanta, A.; Sarkar, P.; Gupta, R., Carbon dioxide adsorption on amine-impregnated mesoporous SBA-15 sorbents: experimental and kinetics study. *Industrial & Engineering Chemistry Research* **2013**, *52* (19), 6480-6491.
47. Ojeda, M.; Mazaj, M.; Garcia, S.; Xuan, J.; Maroto-Valer, M. M.; Logar, N. Z., Novel Amine-impregnated Mesostructured Silica Materials for CO₂ Capture. *Energy Procedia* **2017**, *114*, 2252-2258.
48. Yan, X.; Zhang, L.; Zhang, Y.; Qiao, K.; Yan, Z.; Komarneni, S., Amine-modified mesocellular silica foams for CO₂ capture. *Chemical Engineering Journal* **2011**, *168* (2), 918-924.
49. Yan, X.; Zhang, L.; Zhang, Y.; Yang, G.; Yan, Z., Amine-Modified SBA-15: Effect of Pore Structure on the Performance for CO₂ Capture. *Industrial & Engineering Chemistry Research* **2011**, *50* (6), 3220-3226.
50. Mello, M. R.; Phanon, D.; Silveira, G. Q.; Llewellyn, P. L.; Ronconi, C. M., Amine-modified MCM-41 mesoporous silica for carbon dioxide capture. *Micropor Mesopor Mat* **2011**, *143* (1), 174-179.
51. Jang, H. T.; Park, Y.; Ko, Y. S.; Lee, J. Y.; Margandan, B., Highly siliceous MCM-48 from rice husk ash for CO₂ adsorption. *International Journal of Greenhouse Gas Control* **2009**, *3* (5), 545-549.
52. Stuckert, N. R.; Yang, R. T., CO₂ capture from the atmosphere and simultaneous concentration using zeolites and amine-grafted SBA-15. *Environmental science & technology* **2011**, *45* (23), 10257-10264.
53. Wang, L.; Yang, R. T., Increasing selective CO₂ adsorption on amine-grafted SBA-15 by increasing silanol density. *The Journal of Physical Chemistry C* **2011**, *115* (43), 21264-21272.
54. Wei, J.; Shi, J.; Pan, H.; Zhao, W.; Ye, Q.; Shi, Y., Adsorption of carbon dioxide on organically functionalized SBA-16. *Micropor Mesopor Mat* **2008**, *116* (1-3), 394-399.
55. Knöfel, C.; Descarpentries, J.; Benzaouia, A.; Zeleňák, V.; Mornet, S.; Llewellyn, P.; Hornebecq, V., Functionalised micro-/mesoporous silica for the adsorption of carbon dioxide. *Micropor Mesopor Mat* **2007**, *99* (1-2), 79-85.
56. Choi, S.; Gray, M. L.; Jones, C. W., Amine-tethered solid adsorbents coupling high adsorption capacity and regenerability for CO₂ capture from ambient air. *ChemSusChem* **2011**, *4* (5), 628-635.

57. Sanz, R. I.; Calleja, G.; Arencibia, A.; Sanz-Pérez, E. S., CO₂ uptake and adsorption kinetics of pore-expanded SBA-15 double-functionalized with amino groups. *Energy & fuels* **2013**, *27* (12), 7637-7644.
58. Lin, Z. F.; Wei, J. W.; Geng, L. L.; Mei, D. J.; Liao, L., An Amine Double Functionalized Composite Strategy for CO₂ Adsorbent Preparation using a ZSM-5/KIT-6 Composite as a Support. *Energy Technol-Ger* **2018**, *6* (9), 1618-1626.
59. Demessence, A.; D'Alessandro, D. M.; Foo, M. L.; Long, J. R., Strong CO₂ binding in a water-stable, triazolate-bridged metal-organic framework functionalized with ethylenediamine. *Journal of the American Chemical Society* **2009**, *131* (25), 8784-8786.
60. Yoon, H. C.; Rallapalli, P. B. S.; Beum, H. T.; Han, S. S.; Kim, J.-N., Hybrid Postsynthetic Functionalization of Tetraethylenepentamine onto MIL-101(Cr) for Separation of CO₂ from CH₄. *Energy & Fuels* **2018**, *32* (2), 1365-1373.
61. Szostak, R., Handbook of molecular sieves. 1992. New York: Van Nostrand Reinhold. xvi.
62. Jadhav, P.; Chatti, R.; Biniwale, R.; Labhsetwar, N.; Devotta, S.; Rayalu, S., Monoethanol amine modified zeolite 13X for CO₂ adsorption at different temperatures. *Energy & Fuels* **2007**, *21* (6), 3555-3559.
63. Lin, Y.; Yan, Q.; Kong, C.; Chen, L., Polyethyleneimine incorporated metal-organic frameworks adsorbent for highly selective CO₂ capture. *Scientific reports* **2013**, *3*, 1859.
64. Xian, S.; Xu, F.; Ma, C.; Wu, Y.; Xia, Q.; Wang, H.; Li, Z., Vapor-enhanced CO₂ adsorption mechanism of composite PEI@ ZIF-8 modified by polyethyleneimine for CO₂/N₂ separation. *Chemical Engineering Journal* **2015**, *280*, 363-369.
65. Darunte, L. A.; Oetomo, A. D.; Walton, K. S.; Sholl, D. S.; Jones, C. W., Direct air capture of CO₂ using amine functionalized MIL-101 (Cr). *ACS Sustainable Chemistry & Engineering* **2016**, *4* (10), 5761-5768.
66. Martínez, F.; Sanz, R.; Orcajo, G.; Briones, D.; Yáñez, V., Amino-impregnated MOF materials for CO₂ capture at post-combustion conditions. *Chem Eng Sci* **2016**, *142*, 55-61.
67. Anbia, M.; Hoseini, V., Enhancement of CO₂ adsorption on nanoporous chromium terephthalate (MIL-101) by amine modification. *Journal of Natural Gas Chemistry* **2012**, *21* (3), 339-343.
68. Chen, C.; Kim, S.-S.; Cho, W.-S.; Ahn, W.-S., Polyethyleneimine-incorporated zeolite 13X with mesoporosity for post-combustion CO₂ capture. *Applied Surface Science* **2015**, *332*, 167-171.
69. Su, F.; Lu, C.; Kuo, S.-C.; Zeng, W., Adsorption of CO₂ on Amine-Functionalized Y-Type Zeolites. *Energy & Fuels* **2010**, *24* (2), 1441-1448.
70. Wang, Y.; Du, T.; Qiu, Z.; Song, Y.; Che, S.; Fang, X., CO₂ adsorption on polyethyleneimine-modified ZSM-5 zeolite synthesized from rice husk ash. *Materials Chemistry and Physics* **2018**, *207*, 105-113.
71. Wang, Y.; Du, T.; Song, Y.; Che, S.; Fang, X.; Zhou, L., Amine-functionalized mesoporous ZSM-5 zeolite adsorbents for carbon dioxide capture. *Solid State Sciences* **2017**, *73*, 27-35.
72. Madden, D.; Curtin, T., Carbon dioxide capture with amino-functionalised zeolite-β: A temperature programmed desorption study under dry and humid conditions. *Micropor Mesopor Mat* **2016**, *228*, 310-317.
73. Xu, X.; Zhao, X.; Sun, L.; Liu, X., Adsorption separation of carbon dioxide, methane and nitrogen on monoethanol amine modified β-zeolite. *Journal of Natural Gas Chemistry* **2009**, *18* (2), 167-172.
74. Yang, S.-T.; Kim, J.-Y.; Kim, J.; Ahn, W.-S., CO₂ capture over amine-functionalized MCM-22, MCM-36 and ITQ-2. *Fuel* **2012**, *97*, 435-442.
75. Wang, D.; Ma, X.; Sentorun-Shalaby, C.; Song, C., Development of carbon-based "molecular basket" sorbent for CO₂ capture. *Industrial & engineering chemistry research* **2012**, *51* (7), 3048-3057.
76. Houshmand, A.; Wan Daud, W. M. A.; Shafeeyan, M. S., Exploring potential methods for anchoring amine groups on the surface of activated carbon for CO₂ adsorption. *Separation Science and Technology* **2011**, *46* (7), 1098-1112.

77. Cooper, A. I., Conjugated microporous polymers. *Advanced Materials* **2009**, *21* (12), 1291-1295.
78. Xu, Y.; Jin, S.; Xu, H.; Nagai, A.; Jiang, D., Conjugated microporous polymers: design, synthesis and application. *Chemical Society Reviews* **2013**, *42* (20), 8012-8031.
79. Liu, F.; Wang, S.; Lin, G.; Chen, S., Development and characterization of amine-functionalized hyper-cross-linked resin for CO₂ capture. *New Journal of Chemistry* **2018**, *42* (1), 420-428.
80. Khalil, S. H.; Aroua, M. K.; Daud, W. M. A. W., Study on the improvement of the capacity of amine-impregnated commercial activated carbon beds for CO₂ adsorbing. *Chemical Engineering Journal* **2012**, *183*, 15-20.
81. Gholidoust, A.; Atkinson, J. D.; Hashisho, Z., Enhancing CO₂ adsorption via amine-impregnated activated carbon from oil sands coke. *Energy & Fuels* **2017**, *31* (2), 1756-1763.
82. Bezerra, D. P.; Oliveira, R. S.; Vieira, R. S.; Cavalcante, C. L.; Azevedo, D. C., Adsorption of CO₂ on nitrogen-enriched activated carbon and zeolite 13X. *Adsorption* **2011**, *17* (1), 235-246.
83. Lee, C.; Ong, Y.; Aroua, M.; Daud, W. W., Impregnation of palm shell-based activated carbon with sterically hindered amines for CO₂ adsorption. *Chemical engineering journal* **2013**, *219*, 558-564.
84. Su, F.; Lu, C.; Cnen, W.; Bai, H.; Hwang, J. F., Capture of CO₂ from flue gas via multiwalled carbon nanotubes. *Science of the total environment* **2009**, *407* (8), 3017-3023.
85. Zhao, L.; Bacsik, Z.; Hedin, N.; Wei, W.; Sun, Y.; Antonietti, M.; Titirici, M.-M., Carbon Dioxide Capture on Amine-Rich Carbonaceous Materials Derived from Glucose. *ChemSusChem* **2010**, *3* (7), 840-845.
86. Zhao, Y.; Ding, H.; Zhong, Q., Preparation and characterization of aminated graphite oxide for CO₂ capture. *Applied Surface Science* **2012**, *258* (10), 4301-4307.
87. Liu, F.-Q.; Li, W.; Zhao, J.; Li, W.-H.; Chen, D.-M.; Sun, L.-S.; Wang, L.; Li, R.-X., Covalent grafting of polyethyleneimine on hydroxylated three-dimensional graphene for superior CO₂ capture. *Journal of Materials Chemistry A* **2015**, *3* (23), 12252-12258.
88. Wang, J.; Wang, M.; Zhao, B.; Qiao, W.; Long, D.; Ling, L., Mesoporous Carbon-Supported Solid Amine Sorbents for Low-Temperature Carbon Dioxide Capture. *Industrial & Engineering Chemistry Research* **2013**, *52* (15), 5437-5444.
89. Meng, Y.; Jiang, J.; Gao, Y.; Aihemaiti, A.; Ju, T.; Xu, Y.; Liu, N., Biogas upgrading to methane: Application of a regenerable polyethyleneimine-impregnated polymeric resin (NKA-9) via CO₂ sorption. *Chemical Engineering Journal* **2019**, *361*, 294-303.
90. Chen, Z.; Deng, S.; Wei, H.; Wang, B.; Huang, J.; Yu, G., Polyethylenimine-Impregnated Resin for High CO₂ Adsorption: An Efficient Adsorbent for CO₂ Capture from Simulated Flue Gas and Ambient Air. *ACS Applied Materials & Interfaces* **2013**, *5* (15), 6937-6945.
91. Wang, J.; Wang, M.; Li, W.; Qiao, W.; Long, D.; Ling, L., Application of polyethylenimine-impregnated solid adsorbents for direct capture of low-concentration CO₂. *AIChE Journal* **2015**, *61* (3), 972-980.
92. Liu, F.; Chen, S.; Gao, Y.; Xie, Y., CO₂ adsorption behavior and kinetics on polyethylenimine modified porous phenolic resin. *Journal of Porous Materials* **2017**, *24* (5), 1335-1342.
93. Yin, F.; Peng, P.; Mo, W.; Chen, S.; Xu, T., The preparation of a porous melamine-formaldehyde adsorbent grafted with polyethyleneimine and its CO₂ adsorption behavior. *New Journal of Chemistry* **2017**, *41* (13), 5297-5304.
94. Liu, F.; Chen, S.; Gao, Y.; Xie, Y., Synthesis and CO₂ adsorption behavior of amine-functionalized porous polystyrene adsorbent. *Journal of Applied Polymer Science* **2017**, *134* (28), 45046.
95. Li, W.; Choi, S.; Drese, J. H.; Hornbostel, M.; Krishnan, G.; Eisenberger, P. M.; Jones, C. W., Steam-stripping for regeneration of supported amine-based CO₂ adsorbents. *ChemSusChem* **2010**, *3* (8), 899-903.
96. Belmabkhout, Y.; De Weireld, G.; Sayari, A., Amine-Bearing Mesoporous Silica for CO₂ and H₂S Removal from Natural Gas and Biogas. *Langmuir* **2009**, *25* (23), 13275-13278.

97. Belmabkhout, Y.; Sayari, A., Adsorption of CO₂ from dry gases on MCM-41 silica at ambient temperature and high pressure. 2: Adsorption of CO₂/N₂, CO₂/CH₄ and CO₂/H₂ binary mixtures. *Chem Eng Sci* **2009**, *64* (17), 3729-3735.
98. Belmabkhout, Y.; Serna-Guerrero, R.; Sayari, A., Amine-bearing mesoporous silica for CO₂ removal from dry and humid air. *Chem Eng Sci* **2010**, *65* (11), 3695-3698.
99. Chang, F.-Y.; Chao, K.-J.; Cheng, H.-H.; Tan, C.-S., Adsorption of CO₂ onto amine-grafted mesoporous silicas. *Separation and Purification Technology* **2009**, *70* (1), 87-95.
100. Kishor, R.; Ghoshal, A. K., APTES grafted ordered mesoporous silica KIT-6 for CO₂ adsorption. *Chemical Engineering Journal* **2015**, *262*, 882-890.
101. Ma, X.; Wang, X.; Song, C., "Molecular Basket" Sorbents for Separation of CO₂ and H₂S from Various Gas Streams. *Journal of the American Chemical Society* **2009**, *131* (16), 5777-5783.
102. Yildiz, M. G.; Davran-Candan, T.; Gunay, M. E.; Yildirim, R., CO₂ capture over amine-functionalized MCM-41 and SBA-15: Exploratory analysis and decision tree classification of past data. *J Co2 Util* **2019**, *31*, 27-42.
103. Mafra, L.; Čendak, T.; Schneider, S.; Wiper, P.; Pires, J.; Gomes, J.; Pinto, M., *Amine functionalized porous silica for CO₂/CH₄ separation by adsorption: Which amine and why*. 2017; Vol. 336, p 612.
104. Wei, L.; Gao, Z.; Wang, Y., Integrated two-stage adsorption for selective removal of CO₂ and SO₂ by amine-functionalized SBA-15. *Asia-Pac J Chem Eng* **2017**, *12* (4), 660-670.
105. Goepfert, A.; Zhang, H.; Czaun, M.; May, R. B.; Prakash, G. K. S.; Olah, G. A.; Narayanan, S. R., Easily Regenerable Solid Adsorbents Based on Polyamines for Carbon Dioxide Capture from the Air. *ChemSusChem* **2014**, *7* (5), 1386-1397.
106. Wang, W. J.; Motuzas, J.; Zhao, X. S.; da Costa, J. C. D., Improved CO₂ Sorption in Freeze-Dried Amine Functionalized Mesoporous Silica Sorbent. *Industrial & Engineering Chemistry Research* **2018**, *57* (16), 5653-5660.
107. Psarras, P.; He, J. J.; Wilcox, J., Effect of Water on the CO₂ Adsorption Capacity of Amine-Functionalized Carbon Sorbents. *Industrial & Engineering Chemistry Research* **2017**, *56* (21), 6317-6325.
108. Darunte, L. A.; Walton, K. S.; Sholl, D. S.; Jones, C. W., CO₂ capture via adsorption in amine-functionalized sorbents. *Curr Opin Chem Eng* **2016**, *12*, 82-90.
109. Wang, X.; Chen, L. L.; Guo, Q. J., Development of hybrid amine-functionalized MCM-41 sorbents for CO₂ capture. *Chemical Engineering Journal* **2015**, *260*, 573-581.
110. Palm, D. W.; Enick, R. M.; Vesper, G., Nanoconfined Amine-Functionalized Silicone Oil Sorbents for Rapid CO₂-Capture. *Industrial & Engineering Chemistry Research* **2014**, *53* (42), 16476-16484.
111. Dutcher, B.; Fan, M. H.; Cui, S.; Shen, X. D.; Kong, Y.; Russell, A. G.; McCurdy, P.; Giotto, M., Characterization and stability of a new, high-capacity amine-functionalized CO₂ sorbent. *International Journal of Greenhouse Gas Control* **2013**, *18*, 51-56.
112. Qi, G. G.; Wang, Y. B.; Estevez, L.; Duan, X. N.; Anako, N.; Park, A. H. A.; Li, W.; Jones, C. W.; Giannelis, E. P., High efficiency nanocomposite sorbents for CO₂ capture based on amine-functionalized mesoporous capsules. *Energ Environ Sci* **2011**, *4* (2), 444-452.
113. Yoo, C.-J.; Narayanan, P.; Jones, C. W., Self-supported branched poly (ethyleneimine) materials for CO₂ adsorption from simulated flue gas. *Journal of Materials Chemistry A* **2019**, *7* (33), 19513-19521.
114. Kishor, R.; Ghoshal, A. K., Amine-Modified Mesoporous Silica for CO₂ Adsorption: The Role of Structural Parameters. *Industrial & Engineering Chemistry Research* **2017**, *56* (20), 6078-6087.
115. Sanz-Pérez, E. S.; Arencibia, A.; Calleja, G.; Sanz, R., Tuning the textural properties of HMS mesoporous silica. Functionalization towards CO₂ adsorption. *Micropor Mesopor Mat* **2018**, *260*, 235-244.

116. Dasgupta, S.; Nanoti, A.; Gupta, P.; Jena, D.; Goswami, A. N.; Garg, M. O., Carbon di-oxide removal with mesoporous adsorbents in a single column pressure swing adsorber. *Separation Science and Technology* **2009**, *44* (16), 3973-3983.
117. Goeppert, A.; Czaun, M.; May, R. B.; Prakash, G. S.; Olah, G. A.; Narayanan, S., Carbon dioxide capture from the air using a polyamine based regenerable solid adsorbent. *Journal of the American Chemical Society* **2011**, *133* (50), 20164-20167.
118. Parvazinia, M.; Garcia, S.; Maroto-Valer, M., CO₂ capture by ion exchange resins as amine functionalised adsorbents. *Chemical Engineering Journal* **2018**, *331*, 335-342.
119. Yang, H.; Li, W.; Liu, J.; Sun, Y.; Liu, W., Polyethylenimine-impregnated resins: The effect of support structures on selective adsorption for CO₂ from simulated biogas. *Chemical Engineering Journal* **2019**, *355*, 822-829.
120. Yin, F.; Zhuang, L.; Luo, X.; Chen, S., Simple synthesis of nitrogen-rich polymer network and its further amination with PEI for CO₂ adsorption. *Applied Surface Science* **2018**, *434*, 514-521.
121. Allegue, L. B.; Hinge, J., Biogas upgrading Evaluation of methods for H₂S removal. *Danish Technological, December* **2014**.
122. Huertas, J.; Giraldo, N.; Izquierdo, S., Removal of H₂S and CO₂ from Biogas by Amine Absorption. *Mass Transfer in Chemical Engineering Processes* **2011**, 133-150.
123. Maia, D. C. S.; Cardoso, F. H.; Frareb, L. M.; Gimenes, M. L.; Pereira, N. C., Purification of biogas for energy use. *CHEMICAL ENGINEERING* **2014**, *37*, 643-648.
124. Kakui, T., Dispersion Control of Al₂O₃ Nanoparticles in Ethanol. In *Nanoparticle Technology Handbook*, Elsevier: 2018; pp 727-730.
125. Shi, X.; Zhao, L.; Pei, J.; Ge, L.; Wan, P.; Wang, Z.; Xiao, W., Highly enhancing the characteristics of immobilized thermostable β -glucosidase by Zn²⁺. *Process Biochemistry* **2018**, *66*, 89-96.
126. Balgis, R.; Sago, S.; Anilkumar, G. M.; Ogi, T.; Okuyama, K., Self-organized macroporous carbon structure derived from phenolic resin via spray pyrolysis for high-performance electrocatalyst. *ACS applied materials & interfaces* **2013**, *5* (22), 11944-11950.
127. He, H.; Zhuang, L.; Chen, S.; Liu, H.; Li, Q., Structure design of a hyperbranched polyamine adsorbent for CO₂ adsorption. *Green Chemistry* **2016**, *18* (21), 5859-5869.
128. Witoon, T., Polyethyleneimine-loaded bimodal porous silica as low-cost and high-capacity sorbent for CO₂ capture. *Materials Chemistry and Physics* **2012**, *137* (1), 235-245.
129. Hong, R.; Qian, J.; Cao, J., Synthesis and characterization of PMMA grafted ZnO nanoparticles. *Powder Technology* **2006**, *163* (3), 160-168.
130. Jo, D. H.; Jung, H.; Shin, D. K.; Lee, C. H.; Kim, S. H., Effect of amine structure on CO₂ adsorption over tetraethylenepentamine impregnated poly methyl methacrylate supports. *Separation and Purification Technology* **2014**, *125*, 187-193.
131. Das, A.; Southon, P. D.; Zhao, M.; Kepert, C. J.; Harris, A. T.; D'Alessandro, D. M., Carbon dioxide adsorption by physisorption and chemisorption interactions in piperazine-grafted Ni₂(dobdc)(dobdc= 1, 4-dioxido-2, 5-benzenedicarboxylate). *Dalton Transactions* **2012**, *41* (38), 11739-11744.
132. Wilfong, W. C.; Srikanth, C. S.; Chuang, S. S., In situ ATR and DRIFTS studies of the nature of adsorbed CO₂ on tetraethylenepentamine films. *ACS applied materials & interfaces* **2014**, *6* (16), 13617-13626.
133. Foo, G. S.; Lee, J. J.; Chen, C. H.; Hayes, S. E.; Sievers, C.; Jones, C. W., Elucidation of Surface Species through in Situ FTIR Spectroscopy of Carbon Dioxide Adsorption on Amine-Grafted SBA-15. *ChemSusChem* **2017**, *10* (1), 266-276.
134. Zhang, G.; Zhao, P.; Hao, L.; Xu, Y.; Cheng, H., A novel amine double functionalized adsorbent for carbon dioxide capture using original mesoporous silica molecular sieves as support. *Separation and Purification Technology* **2019**, *209*, 516-527.

135. Sutanto, S.; Dijkstra, J.; Pieterse, J.; Boon, J.; Hauwert, P.; Brilman, D., CO₂ removal from biogas with supported amine sorbents: First technical evaluation based on experimental data. *Separation and purification technology* **2017**, *184*, 12-25.
136. Mokhatab, S.; Poe, W. A.; Mak, J. Y., *Handbook of natural gas transmission and processing: principles and practices*. Gulf Professional Publishing: 2018.
137. Börjesson, P.; Berglund, M. J. B.; bioenergy, Environmental systems analysis of biogas systems— Part I: Fuel-cycle emissions. **2006**, *30* (5), 469-485.
138. Gopalakrishnan, U., Carbon Dioxide Adsorption Using Solid Amine Sorbents. *ProQuest Dissertations and Theses* **2019**, 71.
139. Walas, S. M. *Chemical process equipment; selection and design*; 1988.
140. Wikipedia Carbon dioxide. https://en.wikipedia.org/wiki/Carbon_dioxide (accessed 10/02).
141. AZoM Properties:Silica-Silicon Dioxide (SiO₂). www.azom.com/properties.aspx?ArticleID=1114 (accessed 10/02).
142. Turton, R.; Bailie, R. C.; Whiting, W. B.; Shaeiwitz, J. A., *Analysis, synthesis and design of chemical processes*. Pearson Education: 2008.
143. Alibaba https://www.alibaba.com/product-detail/CFS-302-3-Aminopropyltriethoxysilane-APTES_62015844284.html?spm=a2700.galleryofferlist.normalList.39.52ab94c8n7sN89.
144. Hub, H. Natural Gas Price Today. <https://markets.businessinsider.com/commodities/natural-gas-price> (accessed 10/03).

Appendices

Appendix A: List of Abbreviations and Acronyms

AC – Activated Charcoal

AEAPS - 3-(2-Aminoethylamino)propyldimethoxymethylsilane

AP - 4-Aminopyridine

APTES - 3-Aminopropyltriethoxysilane

APTMS - 3-aminopropyltrimethoxysilane

ATR - Attenuated Total Reflection

b-PEI - Branched Poly(ethylenimine)

BET - Brunauer -Emmett-Teller

BJH - Barrett-Joyner-Halenda

CNG - Compressed Natural Gas

CS - Chemical Scrubbing

DEA - Diethanolamine

DETA - Diethylenetriamine

DRIFTS - Diffuse Reflectance Infrared Fourier Transform Spectroscopy

ED - Ethyl diamine

EDTA - Ethylenediaminetetraacetic acid

FTIR - Fourier-Transform Infrared Spectroscopy

GHG - Greenhouse Gas

HPWS – High Pressure Water Scrubbing

LFG - Landfill Gas

MEA – Monoethanolamine

MMEA - Monomethylethanolamine

MOFs – Metal-organic Frameworks

MS - Membrane Separation

MSW - Municipal Solid Waste

OPS - Organic Physical Scrubbing

PAA - Poly(allylamine)
PEHA - Pentaethylenehexamine
PEI - Poly(ethylenimine)
PSA - Pressure Swing Adsorption
TAEA - Tris(2-aminoethyl)amine
TEPA - Tetraethylenepentamine
TMPTA - Trimethylolpropane triacrylate
TPO - Temperature Programmed Oxidation
TREN - Tris(2-aminoethyl)amine
TSA - Temperature Swing Adsorption
SAS - Supported Amine Sorbent
TETA - Triethylenetetramine
WS - Water Scrubbing

Appendix B: Repeated Experiment Data and Error Analysis

The CO₂ breakthrough experiment using simulated biogas mixture (CH₄/CO₂) was repeated with the 50PEI-HP2MGL sample to examine the repeatability and accuracy of the adsorption capacity measurements. The data from the experiment and the calculated experimental error is summarized in Table B1 and B2 below.

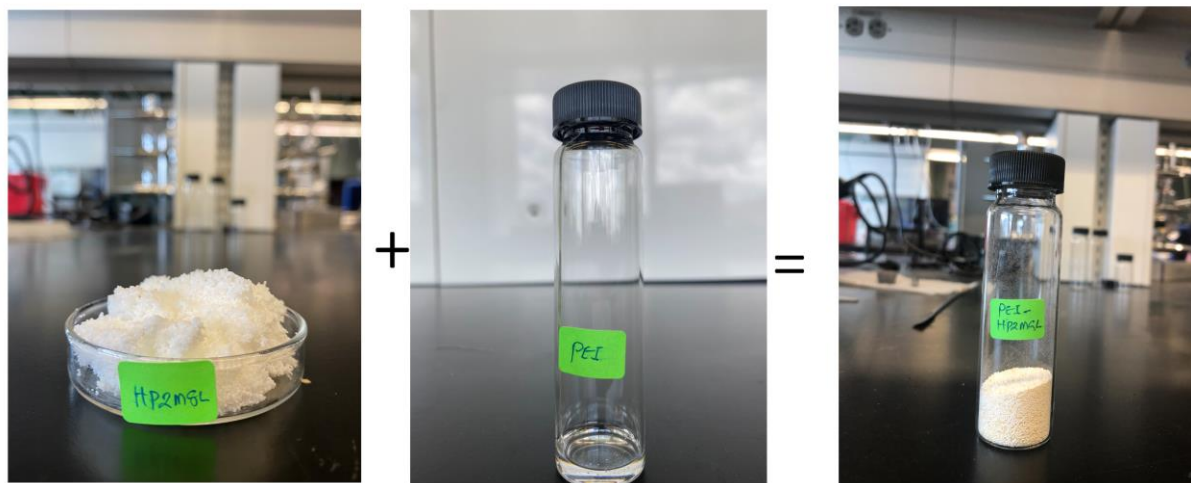
Table B1: 50PEI-HP2MGL repeatability study

50PEI-HP2MGL	Breakthrough Capacity (mmol_{CO2}/g)	Saturated Capacity (mmol_{CO2}/g)
First Experiment	1.45	1.89
Second Experiment	1.44	1.94
Third Experiment	1.46	1.92

Table B2: Experimental Error Calculations

Mean Value	1.92
Standard Deviation	0.03
Mean Standard Deviation	0.01
95% Confidence Level	0.03
Percentage of Error	1.5

Appendix C: Picture of Materials Before and After Modification



Before Wet Impregnation

After Wet Impregnation

Figure C1: Sorbents pictorial views